

General Disclaimer

One or more of the Following Statements may affect this Document

- This document has been reproduced from the best copy furnished by the organizational source. It is being released in the interest of making available as much information as possible.
- This document may contain data, which exceeds the sheet parameters. It was furnished in this condition by the organizational source and is the best copy available.
- This document may contain tone-on-tone or color graphs, charts and/or pictures, which have been reproduced in black and white.
- This document is paginated as submitted by the original source.
- Portions of this document are not fully legible due to the historical nature of some of the material. However, it is the best reproduction available from the original submission.

(NASA-CR-157143) BONDED ORTHOTROPIC STRIPS
WITH CRACKS (Lehigh Univ.) 53 P HC A04/MF
A01 CSCI 20K

N78-24572

G3/39 Unclass
16815

BONDED ORTHOTROPIC STRIPS WITH CRACKS

by

F. Delale and F. Erdogan

June 1978

Lehigh University, Bethlehem, Pa.

The National Aeronautics and Space Administration
Grant No. NGR 39-007-011



BONDED ORTHOTROPIC STRIPS WITH CRACKS

by

F. Delale and F. Erdogan

June 1978

Lehigh University, Bethlehem, Pa.

The National Aeronautics and Space Administration
Grant No. NGR 39-007-011

BONDED ORTHOTROPIC STRIPS WITH CRACKS*

by

F. Delale and F. Erdogan
Lehigh University, Bethlehem, Pa.

ABSTRACT

In this paper the elastostatic problem for a nonhomogeneous plane which consists of two sets of periodically arranged dissimilar orthotropic strips is considered. It is assumed that the plane contains a series of collinear cracks perpendicular to the interfaces and is loaded in tension away from and perpendicular to the cracks. First the problem of cracks fully imbedded into the homogeneous strips is considered. Then the singular behavior of the stresses for two special crack geometries is studied in some detail. The first is the case of a broken laminate in which the crack tips touch the interfaces. The second is the case of cracks crossing the interfaces. An interesting result found from the analysis of the latter which may have an important bearing on a possible delamination fracture initiation at stress-free boundaries in bonded orthotropic materials is that for certain orthotropic material combinations the stress state at the point of intersection of a crack and an interface may be bounded whereas in isotropic materials at this point stresses are always singular. A number of numerical examples are worked out in order to separate the primary material parameters influencing the stress intensity factors and the powers of stress singularity, and to determine the trends regarding the influence of the secondary parameters. Finally, some numerical results are given for the stress intensity factors in certain basic crack geometries and for typical material combinations.

*This work was supported by NASA-Langley under the Grant NGR-39-007-011 and by the National Science Foundation under the Grant ENG77-19127.

1. INTRODUCTION

In considering the failure of a given structural component if the corresponding material is homogeneous and isotropic in its strength and thermomechanical properties, the related fracture process is relatively well-understood and the techniques dealing with such problems are sufficiently well-developed. This is particularly true in the absence of large scale plastic deformations around the dominant flaw from which the fracture failure would develop. On the other hand in composites, particularly in fiber-reinforced laminates, the situation is much more complicated not only because of the nonhomogeneity and anisotropy of the material which make it very difficult to analyze the problem, but also because of the highly nonhomogeneous and nonisotropic distribution of the strength parameter making the development and the application of a proper fracture criterion also very difficult. In such materials it is quite possible that the concept of the progressive growth of a dominant crack with a well-defined leading edge is not an appropriate model for the characterization of gross fracture behavior. Very often the damage zone developing around the dominant flaw is somewhat irregular and diffused and the fracture process is generally governed by a principle of "weakest link", the local fracture propagation being progressive or in discrete steps. Nonetheless, whatever the gross mechanism governing the process of fracture failure in the structure, one may nearly always assume that locally fracture initiation and propagation will take place along the leading edges of the existing flaws where the conditions of the relevant fracture criterion are satisfied. Thus, in order to treat the local fracture phenomenon in composite materials quantitatively, one may need the solution of the mechanics problem for flaws or cracks located at or near the phase boundaries or bimaterial interfaces.

For composites which consist of bonded isotropic materials a wide variety of crack problems have been solved in which

either the asymptotic behavior of the stress state around the points of geometric singularity or the results for a specific crack geometry have been discussed (see, for example, [1] and [2] for review and references). Compared to the isotropic materials, the crack problems for homogeneous or nonhomogeneous anisotropic materials remain to be relatively unexplored. Most of the existing solutions refer to infinite planes [3-7]. The crack problem for an orthotropic strip is considered in [8] and that bonded to two orthotropic half planes is discussed in [9]. The details of the problem for a finite crack located in the neighborhood of or intersecting a bimaterial interface in bonded anisotropic materials do not seem to have been investigated. Even though the problem is rather complicated mostly because of the large number of independent constants entering the analysis, it may be manageable under certain simplifying assumptions. The main assumptions made in this paper are (a) both materials are orthotropic, (b) the nonhomogeneous medium consists of two sets of periodically arranged dissimilar strips having different thicknesses, and (c) the cracks in the strips are collinear, perpendicular to the interfaces, and also periodically arranged (Figure 1). Thus, one can take advantage of the symmetry of the medium and formulate the problem for two bonded strips only. The corresponding problem for isotropic layers or strips were considered in [10] and [11]. In [12] the effect of the thickness and the elastic properties of the adhesive layer on the stress intensity factors in bonded dissimilar isotropic strips was considered.

2. GENERAL FORMULATION OF THE PROBLEM

Consider the plane problem for an orthotropic medium. Referring to, for example, [13] if u and v are the x and y components of the displacement vector, the equations of equilibrium may be expressed as follows:

$$\beta_1 \frac{\partial^2 u}{\partial x^2} + \frac{\partial^2 u}{\partial y^2} + \beta_3 \frac{\partial^2 v}{\partial x \partial y} = 0 ,$$

$$\frac{\partial^2 v}{\partial x^2} + \beta_2 \frac{\partial^2 v}{\partial y^2} + \beta_3 \frac{\partial^2 u}{\partial x \partial y} = 0 , \quad (1a,b)$$

where

$$\beta_1 = \frac{E_{11}}{(1 - \nu_{12}\nu_{21})G_{12}} , \beta_2 = \beta_1 E_{22}/E_{11} , \beta_3 = 1 + \beta_1 \nu_{21} \quad (2)$$

for generalized plane stress, and

$$\beta_1 = b_{11}/G_{12} , \beta_2 = b_{22}/G_{12} , \beta_3 = 1 + b_{12}/G_{12} \quad (3)$$

for plane strain. Here, E_{ij} , ν_{ij} , and G_{ij} , $(i,j) = (1,2,3)$, are the engineering elastic constants, indexes $(1,2,3)$ refer to the (x,y,z) directions, and the matrix (b_{ij}) is given by

$$(b_{ij}) = B = A^{-1} , A = (a_{ij}) , (i,j) = (1,2,3) ;$$

$$a_{ii} = 1/E_{ii} ; a_{ij} = -\nu_{ij}/E_{ii} = a_{ji} , (i \neq j) . \quad (4)$$

The stress-displacement relations are

$$\sigma_{xx} = b_{11} \frac{\partial u}{\partial x} + b_{12} \frac{\partial v}{\partial y} , \sigma_{yy} = b_{12} \frac{\partial u}{\partial x} + b_{22} \frac{\partial v}{\partial y} ,$$

$$\sigma_{xy} = G_{xy} \left(\frac{\partial u}{\partial y} + \frac{\partial v}{\partial x} \right) \quad (5)$$

for plane strain, and

$$\frac{\partial u}{\partial x} = \frac{\sigma_{yy}}{E_{xx}} - \frac{\nu_{xy}}{E_{xx}} \sigma_{yy} , \frac{\partial v}{\partial y} = -\frac{\nu_{yx}}{E_{yy}} \sigma_{xx} + \frac{\sigma_{yy}}{E_{yy}} ,$$

$$\frac{\partial u}{\partial y} + \frac{\partial v}{\partial x} = \sigma_{xy}/G_{xy} \quad (6)$$

for generalized plane stress.

Consider now the periodically arranged two sets of bonded orthotropic strips shown in Figure 1. In addition to the geometric symmetry indicated in the figure, it will be assumed

that the medium is loaded away from the crack region, parallel to the strips, and symmetrical with respect to the x-axis. Thus, the solution of the problem may be obtained by the standard superposition technique, from the viewpoint of fracture the important component being the perturbation solution in which the crack surface tractions are the only external loads. One may note that because of symmetry it is sufficient to consider the problem for one quarter of each strip only. Let (x_1, y) and (x_2, y) be the local axes for the sets of strips 1 and 2 as shown in Figure 1. Let the displacements be expressed in terms of the following Fourier integrals:

$$\begin{aligned} u_j(x_j, y) &= \frac{2}{\pi} \int_0^{\infty} f_j(\alpha, x_j) \cos y\alpha \, d\alpha + \frac{2}{\pi} \int_0^{\infty} g_j(\alpha, y) \sin x_j\alpha \, d\alpha, \\ v_j(x_j, y) &= \frac{2}{\pi} \int_0^{\infty} m_j(\alpha, x_j) \sin y\alpha \, d\alpha + \frac{2}{\pi} \int_0^{\infty} n_j(\alpha, y) \cos x_j\alpha \, d\alpha, \end{aligned} \quad (7a, b)$$

where $j = 1$, and $j = 2$ refer to the strips 1 and 2, respectively. Substituting from (7) into (1) one obtains a system of ordinary differential equations for the unknown functions f_j, \dots, n_j , which are coupled in pairs. Solving these equations we find

$$\begin{aligned} f_j(\alpha, x_j) &= \sum_{k=1}^4 A_{jk}(\alpha) e^{s_{jk} \alpha x_j}, \quad m_j(\alpha, x_j) \\ &= \sum_{k=1}^4 c_{jk} A_{jk}(\alpha) e^{s_{jk} \alpha x_j} \\ g_j(\alpha, y) &= \sum_{k=1}^4 B_{jk}(\alpha) e^{s_{jk} \alpha y / \beta_{j5}}, \quad n_j(\alpha, y) \\ &= \sum_{k=1}^4 d_{jk} B_{jk}(\alpha) e^{s_{jk} \alpha y / \beta_{j5}}, \quad (j=1, 2) \quad (8) \end{aligned}$$

In (8) s_{jk} , $(j=1, 2, k=1, \dots, 4)$ are the roots of the following characteristic equation:

$$s^4 + \beta_{j4}s^2 + \beta_{j5}^2 = 0, \quad s_{j3} = -s_{j1}, \quad s_{j4} = -s_{j2},$$

$$\beta_{j4} = (\beta_{j3}^2 - \beta_{j1}\beta_{j2})/\beta_{j1}, \quad \beta_{j5}^2 = \beta_{j2}/\beta_{j1}, \quad j = 1, 2. \quad (9)$$

The functions A_{jk} and B_{jk} , ($j=1, 2$, $k=1, \dots, 4$) are unknown and the constants c_{jk} and d_{jk} are given by

$$c_{j1} = -c_{j3} = (1 - \beta_{j1}s_{j1}^2)/\beta_{j3}s_{j1},$$

$$c_{j2} = -c_{j4} = (1 - \beta_{j1}s_{j2}^2)/\beta_{j3}s_{j2},$$

$$d_{j1} = -d_{j3} = (s_{j1}^2 - \beta_{j1}\beta_{j5}^2)/\beta_{j3}s_{j1}\beta_{j5},$$

$$d_{j2} = -d_{j4} = (s_{j2}^2 - \beta_{j1}\beta_{j5}^2)/\beta_{j3}s_{j2}\beta_{j5}. \quad (10)$$

The unknown functions A_{jk} and B_{jk} which appear in (8) are determined from the boundary and the continuity conditions of the problem. In addition to the assumed nature of symmetry in loading and geometry, it should be emphasized that in the perturbation problem under consideration the only external loads are the local self-equilibrating crack surface tractions. Consequently, both components of the displacement vector would vanish for $y \rightarrow \pm\infty$, and the x-component of the displacement, u_j ($j=1, 2$) would be zero along the axis of symmetry $x_j = 0$, ($j=1, 2$). Thus, the sixteen conditions which have to be used to determine the unknown functions A_{jk} and B_{jk} ($j=1, 2$; $k=1, \dots, 4$) may be stated as follows:

$$u_j(x_j, y) \rightarrow 0, \quad v_j(x_j, y) \rightarrow 0, \quad (j=1, 2) \text{ for } y \rightarrow \infty, \quad (11)$$

$$u_1(h_1, y) = u_2(-h_2, y), \quad v_1(h_1, y) = v_2(-h_2, y), \quad 0 \leq y < \infty, \quad (12)$$

$$\sigma_{1xx}(h_1, y) = \sigma_{2xx}(-h_2, y), \quad \sigma_{1xy}(h_1, y) = \sigma_{2xy}(-h_2, y), \quad 0 \leq y < \infty, \quad (13)$$

$$u_j(0,y) = 0, \quad \sigma_{jxy}(0,y) = 0, \quad 0 \leq y < \infty, \quad (j=1,2), \quad (14)$$

$$\sigma_{jxy}(x_j,0) = 0, \quad |x_j| < h_j, \quad (j=1,2), \quad (15)$$

$$\sigma_{1yy}(x_1,0) = p_1(x_1), \quad |x_1| < a,$$

$$v_1(x_1,0) = 0, \quad a < |x_1| < h_1, \quad (16a,b)$$

$$\sigma_{2yy}(x_2,0) = p_2(x_2), \quad c < |x_2| < d,$$

$$v_2(x_2,0) = 0, \quad 0 < |x_2| < c, \quad d < |x_2| < h_2 \quad (17a,b)$$

In (9) it may arbitrarily be assumed that

$$\operatorname{Re}(s_{j1}) > 0, \quad \operatorname{Re}(s_{j2}) > 0, \quad (j=1,2). \quad (18)$$

From (7), (8), (11) and (18) it therefore follows that

$$B_{j1}(\alpha) = 0, \quad B_{j2}(\alpha) = 0, \quad (j=1,2). \quad (19)$$

Ten of the remaining twelve unknown functions may be eliminated by using the homogeneous conditions (12-15) in (8), (7) and (6). The last two unknown functions are then determined from the mixed boundary conditions (16) and (17). The problem may be reduced to a pair of integral equations by defining

$$\frac{\partial}{\partial x_j} v_j(x_j,0) = \phi_j(x_j), \quad 0 < |x_j| < h_j, \quad (j=1,2), \quad (20)$$

and by replacing the conditions (16) and (17) by (20). Thus all the unknown functions A_{jk} and B_{jk} may easily be expressed in terms of the new unknown functions ϕ_1 and ϕ_2 . We now observe that part of the mixed conditions, namely (16b) and (17b) is equivalent to

$$\phi_1(x_1) = 0, \quad a < |x_1| < h_1; \quad \int_{-a}^a \phi_1(x_1) dx_1 = 0, \quad (21)$$

$$\phi_2(x_2) = 0, \quad 0 < |x_2| < c, \quad d < |x_2| < h_2; \quad \int_c^d \phi_2(x_2) dx_2 = 0. \quad (22)$$

Through equations (8), (7), and (6), substituting the results into the conditions (16a) and (16b) we obtain two integral

equations to determine ϕ_1 and ϕ_2 .

Because of the large number of elastic constants and unknown functions the process of deriving the integral equations is rather complicated and lengthy. However, the technique is straightforward and is quite similar to that followed in [10] and [11]. Therefore, the details of the derivations will not be given in this paper. As in [10], it can be shown that the integral equations are singular and may be expressed as follows:

$$\int_{L_1} \left[\frac{1}{\pi} \left(\frac{1}{t-x_1} + \frac{1}{t+x_1} \right) + k_{11}(x_1, t) - k_{11}(x_1, -t) \right] \phi_1(t) dt + \int_{L_2} [k_{12}(x_1, t) - k_{12}(x_1, -t)] \phi_2(t) dt = \frac{1}{\mu_1} p_1(x_1) ,$$

$$x_1 \in L_1 ,$$

$$\int_{L_1} [k_{21}(x_2, t) - k_{21}(x_2, -t)] \phi_1(t) dt + \int_{L_2} \left[\frac{1}{\pi} \left(\frac{1}{t-x_2} + \frac{1}{t+x_2} \right) + k_{22}(x_2, t) - k_{22}(x_2, -t) \right] \phi_2(t) dt = \frac{1}{\mu_2} p_2(x_2) ,$$

$$x_2 \in L_2 , \quad (23a, b)$$

where L_1 and L_2 refer to the cracks on ($y=0$, $0 \leq x_1 < h_1$) and ($y=0$, $0 \leq x_2 < h_2$) in the strips 1 and 2, respectively, and

$$\mu_1 = 2E_{1yy} \gamma_{14} / (1 - \nu_{1xy} \nu_{1yx}) , \quad \mu_2 = 2E_{2yy} \gamma_{14}^* / (1 - \nu_{2xy} \nu_{2yx}) . \quad (24)$$

In deriving the integral equations one needs to define in a systematic fashion a large number of elastic constants and intermediate functions. Therefore, in order to conserve space the definitions leading to the expressions of the kernels k_{ij} , ($i, j=1, 2$), and the constants γ_{14} and γ_{14}^* , and to the relationships between the functions A_{jk} , B_{jk} and ϕ_i will also

be omitted in this paper^(*). These definitions and the details of certain derivations may be found in [14] for the group of orthotropic materials which would give a characteristic equation having only real roots $s_{jk}, (j=1,2; k=1,\dots,4)$ (defined henceforth as the orthotropic materials of type I), and in [15] for materials which would give a characteristic equation with only complex conjugate roots (defined as the orthotropic materials of type II)^(**).

The kernels k_{ij} which appear in (23) are of the following form:

$$k_{ij}(x_i, t) = \int_0^\infty K_{ij}(x_i, t, \alpha) d\alpha, \quad (i, j=1, 2) \quad (25)$$

Examining the behavior of K_{ij} for $\alpha \rightarrow 0$ it can be shown that

$$K_{ij} = \frac{c_{ij}}{\alpha} + O(1) \quad (26)$$

where c_{ij} are known constants. Even though this may imply divergent kernels, by writing

$$\begin{aligned} \int_{L_j} k_{ij}(x_i, t) \phi_j(t) dt &= \int_{L_j} \phi_j dt \int_0^\infty (K_{ij} - \frac{c_{ij}}{\alpha}) d\alpha \\ &\quad + \int_{L_j} \phi_j dt \int_0^\infty \frac{c_{ij}}{\alpha} d\alpha, \quad (i, j=1, 2) \end{aligned} \quad (27)$$

and by using single-valuedness conditions (see (21), (22))

$$\int_{L_j} \phi_j(t) dt = 0, \quad (j=1, 2) \quad (28)$$

it is seen that the singularity at $\alpha = 0$ may easily be removed. Also, by examining the behavior of the integrands $K_{ij}, (i, j=1, 2)$ for $\alpha \rightarrow \infty$ it can be shown that they decay exponentially provided the series of collinear cracks L_i ($i=1, 2$) are fully imbedded in

(*) Note that the constant γ_{14} is the same as the constants m_{14} and r_{14} defined in [8] (eqs. 14, 16 and 19) and the constants defined in (24) correspond to $4\mu/(1+\kappa)$ for the isotropic materials.

(**) In practice, since β_{j4} in the characteristic equation (9) appears to be always a negative quantity, the third type of material giving four pure imaginary roots is not a realistic one.

the homogeneous strips (i.e., they do not touch or intersect the bimaterial interfaces). Thus, in solving the integral equations (23), k_{ij} may be treated as Fredholm kernels. In this problem since the kernels of the integral equations have only a Cauchy type singularity, the functions ϕ_i would have a square root singularity at the end points L_i and the equations may easily be solved by normalizing the intervals and by using the technique described, for example, in [16]. After solving the integral equations, the stress intensity factors may be obtained in terms of the functions ϕ_i . For example, let Figure 1 describe the crack geometry, i.e., let $L_1=(0,a)$, $L_2=(c,d)$; then, the stress intensity factors may be defined and obtained as follows [8]:

$$\begin{aligned} k(a) &= \lim_{t \rightarrow a} \sqrt{2(t-a)} \sigma_{1yy}(t,0) = -\lim_{t \rightarrow a} \mu_1 \sqrt{2(a-t)} \phi_1(t) , \\ k(c) &= \lim_{t \rightarrow c} \sqrt{2(c-t)} \sigma_{2yy}(t,0) = \lim_{t \rightarrow c} \mu_2 \sqrt{2(t-c)} \phi_2(t) , \\ k(d) &= \lim_{t \rightarrow d} \sqrt{2(t-d)} \sigma_{2yy}(t,0) = -\lim_{t \rightarrow d} \mu_2 \sqrt{2(d-t)} \phi_2(t) . \end{aligned} \quad (29a-c)$$

3. CRACK TOUCHING THE INTERFACE

Two limiting cases of the problem discussed in the previous section are physically important and mathematically interesting. These are the cases of a broken laminate corresponding to a crack touching the interface (e.g., $a=h_1$, $d<h_2$, Figure 1), and a crack intersecting the interface (e.g., $a=h_1$, $d=h_2$, $0<c<h_2$, Figure 1). For example, referring to Figure 1, let $a=h_1$ and $d<h_2$. In this case it may be shown that as $\alpha \rightarrow \infty$ and for $-h_1 \leq (x_1, t) \leq h_1$, $c \leq (|x_2|, |t|) \leq d$ the integrands K_{12} , K_{21} , and K_{22} in (25) decay exponentially. Therefore, the kernels k_{12} , k_{21} , and k_{22} are bounded in their respective closed domains. On the other hand for $x_1 \rightarrow h_1$, $t \rightarrow h_1$ the exponential decay in $K_{11}(x_1, t,)$ disappears, indicating that $k_{11}(x_1, t)$ may contain terms which become singular as x_1 and t approach

the end point h_1 simultaneously. These singular terms can be separated by studying the asymptotic behavior of the integrals given by (25) (see [16] for the technique and [10], [14], [17] and [18] for the application). To give an idea about the nature of these additional singular kernels let

$$k_{11}(x_1, t) = k_{11s}(x_1, t) + k_{11f}(x_1, t) \quad , \quad 0 \leq (x_1, t) \leq h_1 \quad , \quad (30)$$

where k_{11s} represents the singular terms and k_{11f} is bounded in the related closed domain. Let the material be of type I with the real roots (see equation 9)

$$s_{11} = \omega_1 > 0 \quad , \quad s_{12} = \omega_2 > 0 \quad , \quad s_{13} = -\omega_1 \quad , \quad s_{14} = -\omega_2 \quad . \quad (31)$$

Then the asymptotic analysis of (25) would give

$$\begin{aligned} \pi k_{11s}(x_1, t) = & \lambda_{85} \frac{(h_1 - t)\beta_{15}/\omega_1 + h_1\omega_1}{[(h_1 - t)\beta_{15}/\omega_1 + h_1\omega_1]^2 - (\omega_1 x_1)^2} \\ & \lambda_{86} \frac{(h_1 - t)\beta_{15}/\omega_1 + \omega_2 h_1}{[(h_1 - t)\beta_{15}/\omega_1 + h_1\omega_2]^2 - (\omega_2 x_1)^2} \\ & \lambda_{87} \frac{(h_1 - t)\beta_{15}/\omega_2 + h_1\omega_1}{[(h_1 - t)\beta_{15}/\omega_2 + h_1\omega_1]^2 - (\omega_1 x_1)^2} \\ & \lambda_{88} \frac{(h_1 - t)\beta_{15}/\omega_2 + h_1\omega_2}{[(h_1 - t)\beta_{15}/\omega_2 + h_1\omega_2]^2 - (\omega_2 x_1)^2} \quad , \\ & 0 \leq (x_1, t) \leq h_1 \quad (32) \end{aligned}$$

where $\lambda_{85}, \dots, \lambda_{88}$ are known constants and depend on the elastic properties of the materials only [14].

Together with $1/(t-x_1)$, k_{11s} gives a generalized Cauchy kernel. Substituting from (30) into (23) and adopting the crack geometry shown in Figure 1 (with $a=h_1$), the dominant part of (23) may be expressed as

$$\begin{aligned} \frac{1}{\pi} \int_{-h_1}^{h_1} \left[\frac{1}{t-x_1} + \pi k_{11s}(x_1, t) \right] \phi_1(t) dt &= P_1(x_1) \quad , \quad -h_1 < x_1 < h_1 \quad , \\ \frac{1}{\pi} \int_c^d \frac{1}{t-x_2} \phi_2(t) dt &= P_2(x_2) \quad , \quad c < x_2 < d \quad , \end{aligned} \quad (33a, b)$$

where the bounded functions P_1 and P_2 contain all the non-singular terms in (23). It is clear that the solution of (33b) is of the form

$$\phi_2(t) = F_2(t) [(t-c)(d-t)]^{-1/2} \quad , \quad c < t < d \quad (34)$$

giving the stress intensity factors as defined in (29). The singular behavior of the solution of (33a) may be studied by letting

$$\phi_1(t) = F_1(t) / (h_1^2 - t^2)^\gamma \quad , \quad 0 < \text{Re}(\gamma) < 1 \quad , \quad -h_1 < t < h_1 \quad (35)$$

and by using the function-theoretic method described in, for example, [16]. Thus, if we define the following sectionally holomorphic function

$$G(z) = \frac{1}{\pi} \int_{-h_1}^{h_1} \frac{\phi_1(t)}{t-z} dt \quad , \quad (x_1 = \text{Re}(z)) \quad , \quad (36)$$

by using (35) the asymptotic analysis of (36) gives

$$\begin{aligned} G(z) &= \frac{F_1(-h_1) e^{i\pi\gamma}}{(2h_1)^\gamma \sin\pi\gamma} \frac{1}{(z+h_1)^\gamma} - \frac{F_1(h_1)}{(2h_1)^\gamma \sin\pi\gamma} \frac{1}{(z-h_1)^\gamma} + G_0(z) \quad , \\ |G_0(z)| &< \frac{C_0}{|z \mp h_1|^{\gamma_0}} \quad , \quad \gamma_0 < \text{Re}(\gamma) \quad , \end{aligned} \quad (37a, b)$$

where C_0 and γ_0 are real constants. Now, substituting from (37) and (32) into (33a), we obtain the following characteristic equation to determine the unknown constant γ :

$$-2\cos\pi\gamma + \lambda_{85} \frac{\omega_1^{1-2\gamma}}{\beta_{15}^{1-\gamma}} + \lambda_{86} \frac{\omega_1^{1-\gamma}}{\omega_2 \beta_{15}^{1-\gamma}} + \lambda_{87} \frac{\omega_2^{1-\gamma}}{\omega_1 \beta_{15}^{1-\gamma}} + \lambda_{88} \frac{\omega_2^{1-2\gamma}}{\beta_{15}^{1-\gamma}} = 0, \quad (38)$$

where, again the material type I is assumed. It can be shown that for all material combinations (38) may have only one root in the strip $0 < \text{Re}(\gamma) < 1$ and this root is always real. It can also be shown that as the orthotropic material constants tend to those for a pair of isotropic materials, the root γ obtained from (38) approaches the root of the corresponding isotropic characteristic equation given, for example, in [10] or [18].

For this crack geometry the "stress intensity factor" may be defined in terms of the cleavage stress σ_{2yy} in the neighboring material which, from the fracture viewpoint, is the most important stress component. To calculate this we note that (23b) gives the expression for $\sigma_{2yy}(x_2, 0)$ for $-h_2 \leq x_2 \leq h_2$, that is in the uncracked as well as in the cracked portion of the strip. We also note that in the neighborhood of $|x_2| = h_2$ the singular behavior of σ_{2yy} will be governed by the density function ϕ_1 and the singular part of the kernel k_{21} . As in K_{11} , it may be shown that for $\alpha \rightarrow \infty$, $t \rightarrow h_1$, $x_2 \rightarrow h_2$, the exponential decay in K_{21} disappears, indicating that $k_{21}(x_2, t)$ may contain terms which become singular as x_2 and t go to the end point simultaneously. If we again let

$$k_{21}(x_2, t) = k_{21s}(x_2, t) + k_{21f}(x_2, t), \quad (39)$$

the singular part of the kernel may be separated and may be expressed as

$$\begin{aligned}
\pi k_{21s}(x_2, t) = & \lambda_{101} \frac{(h_1 - t)\beta_{15}/\omega_1 + \alpha_1 h_2}{[(h_1 - t)\beta_{15}/\omega_1 + \alpha_1 h_2]^2 - (\alpha_1 x_2)^2} \\
& + \lambda_{102} \frac{(h_1 - t)\beta_{15}/\omega_1 + \alpha_2 h_2}{[(h_1 - t)\beta_{15}/\omega_1 + \alpha_2 h_2]^2 - (\alpha_2 x_2)^2} \\
& + \lambda_{103} \frac{(h_1 - t)\beta_{15}/\omega_2 + \alpha_1 h_2}{[(h_1 - t)\beta_{15}/\omega_2 + \alpha_1 h_2]^2 - (\alpha_1 x_2)^2} \\
& + \lambda_{104} \frac{(h_1 - t)\beta_{15}/\omega_2 + \alpha_2 h_2}{[(h_1 - t)\beta_{15}/\omega_2 + \alpha_2 h_2]^2 - (\alpha_2 x_2)^2},
\end{aligned}$$

$$0 \leq |t| \leq h_1, \quad 0 \leq |x_2| \leq h_2 \quad (40)$$

where α_1 and α_2 are the positive roots s_{21} and s_{22} of the characteristic equation (9) expressed for the strip 2 and the constants λ are defined in [14]. Thus, for the purpose of analyzing the singularity σ_{2yy} may be expressed as

$$\sigma_{2yy}(x_2, 0) = \mu_2 \int_{-h_1}^{h_1} k_{21s}(x_2, t) \phi_1(t) dt + p_{20}(x_2) \quad (41)$$

where p_{20} contains all the nonsingular terms. Upon substituting from (35) and (40) into (41), the asymptotic analysis gives

$$\sigma_{2yy}(x_2, 0) = \frac{k(h_1)}{2\gamma(x_2 + h_2)^\gamma} + \sigma_0(x_2) \quad (42)$$

where $\sigma_0(x_2)$ remains bounded as $x_2 \rightarrow -h_2$ and the "stress intensity factor" $k(h_1)$ is found to be

$$k(h_1) = \mu_2^* \lim_{t \rightarrow h_1} 2^\gamma (h_1 - t)^{\gamma} \phi_1(t) ,$$

$$\begin{aligned} \mu_2^* = \frac{\mu_2}{\sin \pi \gamma} & \left[\lambda_{101} \alpha_1^{-\gamma} \left(\frac{\omega_1}{\beta_{15}} \right)^{1-\gamma} + \lambda_{102} \alpha_2^{-\gamma} \left(\frac{\omega_1}{\beta_{15}} \right)^{1-\gamma} \right. \\ & \left. + \lambda_{103} \alpha_1^{-\gamma} \left(\frac{\omega_2}{\beta_{15}} \right)^{1-\gamma} + \lambda_{104} \alpha_2^{-\gamma} \left(\frac{\omega_2}{\beta_{15}} \right)^{1-\gamma} \right] . \end{aligned} \quad (43)$$

4. CRACK CROSSING THE INTERFACE

Consider now the case of a crack crossing the interface. In this problem the integral equations (23) are still valid with the two end points of the cuts L_1 and L_2 joining at the interface. For example, referring to Figure 1, let $a = h_1$, $d = h_2$, and $c > 0$. In this case at the end point $x_1 = h_1$ or $x_2 = h_2$ all four kernels $k_{ij}(x_i, t)$ will have singular terms. The singular parts k_{11s} and k_{21s} coming from k_{11} and k_{21} are separated and are given by (32) and (40). Quite similar expressions may easily be obtained for k_{12s} and k_{22s} [14,15]. The dominant part of the system of singular integral equations may then be expressed as

$$\sum_{j=1}^2 \int_{L_j} \left[\frac{1}{\pi} \frac{\delta_{ij}}{t-x_j} + k_{ijs}(x_j, t) \right] \phi_j(t) dt = Q_i(x_i) ,$$

$$L_1 = (-h_1, h_1) , L_2 = (c, h_2) , x_i \in L_i , (i=1,2) \quad (44)$$

where in the analysis the symmetry condition of $\phi_2(x_2) = -\phi_2(-x_2)$ is used. If we now let

$$\phi_1(t) = \frac{F_1(t)}{(h_1^2 - t^2)^\beta} , \quad \phi_2(t) = \frac{F_2(t)}{(h_2 - t)^\beta (t - c)^\delta} ,$$

$$0 < \operatorname{Re}(\beta, \delta) < 1 , \quad (45a, b)$$

and define the following sectionally holomorphic functions

$$G_1(z) = \frac{1}{\pi} \int_{-h_1}^{h_1} \frac{\phi_1(t)}{t - z} dt , \quad G_2(z) = \frac{1}{\pi} \int_c^{h_2} \frac{\phi_2(t)}{t - z} dt , \quad (46a, b)$$

The asymptotic expressions for G_1 and G_2 may be obtained as [16]

$$G_1(z) = \frac{1}{(2h_1)^\beta \sin \pi \beta} \left[\frac{F_1(-h_1) e^{i\pi \beta}}{(z + h_1)^\beta} - \frac{F_1(h_1)}{(z - h_1)^\beta} \right] + G_{10}(z) ,$$

$$G_2(z) = \frac{F_2(c) e^{i\pi \delta}}{(h_2 - c)^\beta \sin \pi \delta} \frac{1}{(z - c)^\delta} - \frac{F_2(h_2)}{(h_2 - c)^\delta \sin \pi \beta} \frac{1}{(z - h_2)^\beta} + G_{20}(z) , \quad (47a, b)$$

where G_{j0} ($j = 1, 2$) has a behavior similar to that of $G_0(z)$ which is given by (37b). Noting that outside their respective cuts G_1 and G_2 are holomorphic, substituting from (47) into (44), and following the procedure outlined, for example, in [16] (see, also [14] for details) we obtain

$$F_2(c) \cot \pi \delta = 0 \quad (48)$$

$$\sum_{j=1}^2 f_{ij}(\beta) F_j(h_j) = 0 , \quad (i=1, 2) , \quad (49)$$

where the coefficients in the functions $f_{ij}(\beta)$ depend on the elastic constants of the two strips only and are given in [14]. Since $F_2(c)$ and $F_j(h_j)$, ($j=1, 2$) are nonzero constants, (48)

gives the known result $\delta = 1/2$ and from (49) we obtain the following characteristic equation to determine the power of singularity β :

$$\Delta(\beta) = |f_{ij}(\beta)| = 0 \quad , \quad (i,j=1,2) \quad , \quad 0 < \text{Re}(\beta) < 1 \quad . \quad (50)$$

It is also important to note that the end point values $F_1(h_1)$ and $F_2(h_2)$ are not independent and are related by

$$F_2(h_2) = -F_1(h_1)f_{11}(\beta)/f_{12}(\beta) \quad (51)$$

where β is the root of (50). An additional condition such as (51) is necessary to obtain a unique solution for the system of integral equations (23), since in this case there is only one single-valuedness condition which has to be satisfied by the displacement derivatives ϕ_1 and ϕ_2 , namely

$$\int_c^{h_2} \phi_2(t) dt + \int_{-h_1}^{h_1} \phi_1(t) dt + \int_{-h_2}^{-c} \phi_2(t) dt = 0 \quad . \quad (52)$$

A systematic study of (50) indicates that for all material combinations the characteristic equations may have either no root or only a single real root in the strip $0 < \text{Re}(\beta) < 1$. Also, $\beta = 0$ is always a root and there are no other roots with $\text{Re}(\beta) = 0$. In the foregoing analysis only the possibility of a power singularity is investigated. The results show that for certain material combinations (50) indeed has no root in $0 < \text{Re}(\beta) < 1$, implying that for these materials at the intersection of the crack and the interface the stress state would be bounded. However, this analysis does not prove that in such cases there may not be a weaker, namely a logarithmic singularity. To

investigate this question in (45) we let $\beta = 0$ and substitute the result into (46). We would then obtain the following asymptotic relations:

$$G_1(z) = \frac{F_1(h_1)}{\pi} \log(z-h_1) - \frac{F_1(-h_1)}{\pi} \log(z+h_1) + G_{11}(z) ,$$

$$G_2(z) = \frac{F_2(c)e^{i\pi\delta}}{\sin\pi\delta} \frac{1}{(z-c)^\delta} + \frac{F_2(h_2)}{\pi(h_2-c)^\delta} \log(z-h_2) + G_{21}(z) , \quad (53)$$

where G_{11} and G_{21} are bounded near and at the end points $z = \pm h_j$ and G_{21} has a behavior similar to (37b) in the neighborhood of $z = c$. Substituting now from (53) into the integral equations (44) we obtain

$$F_2(c) \cot\pi\delta = 0 , \quad (54)$$

$$\log(h_i - x_i) \sum_{j=1}^2 g_{ij} F_j(h_j) = R_i(x_i) , \quad (i=1,2) \quad (55)$$

where R_1 and R_2 are bounded functions and the constants g_{ij} , $(i,j=1,2)$ depend on the elastic constants only. Equation (54) again gives the known result $\delta = 1/2$. For (55) to be valid at $x_i = h_i$, $(i=1,2)$ the coefficient of singular terms must vanish, or we must have

$$\sum_{j=1}^2 g_{ij} F_j(h_j) = 0 , \quad (i=1,2) . \quad (56)$$

Since $F_j(h_j)$, $(j=1,2)$ are nonzero constants, from (56) it follows that

$$|g_{ij}| = 0 \quad (57)$$

To show (57) analytically seems to be impossible. However, a systematic numerical analysis indicates that for the material combinations having $\beta = 0$ as the only acceptable power singularity (57) is indeed satisfied identically. Furthermore, these studies also show that (56) always gives

$$\frac{\phi_1(h_1)}{\phi_2(h_2)} = \frac{\phi_1(h_1)}{\phi_2(-h_2)} = -1 \quad (58)$$

The result expressed by (58) meaning that in the composite medium the derivative of the crack surface displacement is continuous at the interface is, of course, the physically expected result.

For the pair of materials in which (50) has a root in $0 < \beta < 1$, at the point ($y=0$, $x_1=h_1$ or $x_2=-h_2$) the stress state will be singular. At this point, since the important stress components are the normal and shear stresses on the interface, we may directly analyze the singular behavior of these stresses. To do this one has to go back to the original formulation of the problem and express these stresses in terms of the density functions ϕ_1 and ϕ_2 . Thus, after somewhat lengthy but straightforward analysis we find [14,15]

$$\frac{1}{\mu_1} \sigma_{1xi}(h_1, y) = \frac{1}{\pi} \sum_{j=1}^2 \int_{L_j} h_{ij}(y, s) \phi_j(s) ds, \quad (i=x, y),$$

$$L_1 = (-h_1, h_1), \quad L_2 = (c, h_2) \quad (59)$$

Studying the asymptotic behavior of the kernels h_{ij} it can be shown that as $y \rightarrow 0$, $s \rightarrow h_1$ in $-h_1 < s < h_1$, and $s \rightarrow h_2$ in $c < s < h_2$ simultaneously the kernels become unbounded. By expressing

$$h_{ij}(y, s) = h_{ijf}(y, s) + h_{ijs}(y, s),$$

the singular parts h_{ijs} of these kernels can again be separated. For example, for $h_{x1s}(y, s)$ we obtain

$$\begin{aligned} 2\gamma_{13}h_{x1s}(y, s) = & \frac{(h_1+s)\gamma_1/2}{(h_1+s)^2+(\omega_1 y/\beta_{15})^2} - \frac{(h_1-s)\gamma_1/2}{(h_1-s)^2+(\omega_1 y/\beta_{15})^2} \\ & - \frac{(h_1+s)\gamma_2\gamma_{11}/2\gamma_{12}}{(h_1+s)^2+(\omega_2 y/\beta_{15})^2} + \frac{(h_1-s)\gamma_2\gamma_{11}/2\gamma_{12}}{(h_1-s)^2+(\omega_2 y/\beta_{15})^2} \\ & + \frac{\gamma_3\lambda_{81}+\gamma_4\lambda_{82}}{\lambda_{80}} \frac{(h_1-s)\beta_{15}/\omega_1}{[(h_1-s)\beta_{15}/\omega_1]^2+y^2} \\ & + \frac{\gamma_3\lambda_{83}+\gamma_4\lambda_{84}}{\lambda_{80}} \frac{(h_1-s)\beta_{15}/\omega_2}{[(h_1-s)\beta_{15}/\omega_2]^2+y^2}, \quad (60) \end{aligned}$$

where the definition of the material constants γ and λ as well as the expressions for the remaining functions h_{x2s} , h_{y1s} , and h_{y2s} may be found in [14] and [15].

If the materials are such that the stress state at $(y=0, x_1=h_1)$ is singular, i.e., $0 < \beta < 1$, then one can again define ϕ_i and G_i , ($i=1,2$) as in (45) and (46) and obtain (47). Now observing that outside the cuts L_1 and L_2 , specifically along the y -axis G_1 and G_2 are holomorphic, one can use (47)

to evaluate the singular terms in (59) (see, for example [16-18]). It can then be shown that

$$\sigma_{1xx}(h_1, y) = \frac{k_{xx}}{y^\beta} + \sigma_0(y) \quad , \quad (y > 0) \quad ,$$

$$\sigma_{1xy}(h_1, y) = \frac{k_{xy}}{y^\beta} + \tau_0(y) \quad , \quad y > 0 \quad (61a, b)$$

where the "stress intensity factors" may be expressed in terms of the density functions as follows:

$$k_{xx} = \mu_{xx} \lim_{t \rightarrow h_1} (h_1 - t)^\beta \phi_1(t) \quad ,$$

$$k_{xy} = \mu_{xy} \lim_{t \rightarrow h_1} (h_1 - t)^\beta \phi_1(t) \quad . \quad (62a, b)$$

The constants μ_{xx} and μ_{xy} are known functions of the elastic constants and may be found in [14] and [15].

For the material combinations in which ϕ_1 and ϕ_2 have no singularity at $x_1 = h_1$, $x_2 = -h_2$, (i.e., if $\beta = 0$ is the only acceptable root of (50)), since the kernels h_{ij} have singular parts of the form (60), from (59) it is not at all obvious that the stresses too would be bounded at the point $(y=0, x_1=h_1)$. This question can be examined by substituting from (45) with $\beta = 0$, $\delta = 1/2$ into (59) and by going through a routine asymptotic analysis, which yields

$$\sigma_{1xx}(h_1, y) = F_1(h_1) \theta_{xx} \log y + C(y)$$

$$\sigma_{1xy}(h_1, y) = D(y) \quad (63a, b)$$

where $C(y)$ and $D(y)$ are bounded functions. It turns out that in all material combinations for which $\beta = 0$, the constant σ_{xx} is identically zero; therefore, the stresses are bounded.

Considering the fact that in isotropic materials the stress state at the intersection of an interface and a crack is always singular (i.e., $\beta > 0$), from the viewpoint of delamination or debonding fracture the practical importance of the possibility of having bounded stresses at such locations in designing with certain orthotropic materials needs no elaboration.

5. NUMERICAL SOLUTION

In this paper the numerical results are obtained for several specific types of crack geometries. In the first group of solutions it is assumed that the cracks are fully imbedded in homogeneous strips and (see Figure 1)

$$a < h_1, \quad c = 0, \quad d = b < h_2. \quad (64)$$

The single crack, $a = 0, b \neq 0$ or $a \neq 0, b = 0$ is considered as a special case. In this problem the integral equations (23) are solved by using the Gauss-Chebyshev integration method [16] with $L_1 = (-a, a)$, $L_2 = (-b, b)$ and under the single-valuedness conditions (28). The stress intensity factors are then obtained from (29a) and (29c) with $d = b$.

In the second group of solutions it is assumed that $a = h_1$ and $0 < b < h_2$. In this case the Gauss-Jacobi integration method is used to solve the integral equations. The details of the

numerical method may be found in [16,4 or 18]. After obtaining the density functions the stress intensity factors are calculated from (29c) (with $d=b$) and (43).

In the third group of solutions it is assumed that the crack crosses the interface, that is, $a = h_1$, $d = h_2$, $0 < c < h_2$ (Figure 1). In this case for $\beta > 0$, the integral equations (23) are solved by substituting from (45) and by using the Gauss-Jacobi integration method. Here the additional conditions are (51) and (52). After obtaining ϕ_1 and ϕ_2 the stress intensity factors are determined from (29b) and (62) (see again [16], [14] or [18] for numerical procedure).

6. RESULTS

The elastic properties of the materials used in the numerical examples are shown in Table 1. Materials 3, 4, and 6 are basically isotropic and the remaining materials are orthotropic. For the materials 1 through 8 the roots of the characteristic equation (9) are real, meaning that they are of type I. Materials 9 and 10 are of type II for which (9) has complex conjugate roots. The numerical results given in this paper are all for the case of plane stress. Table 2 shows the material combinations used in the numerical analysis. The table also shows the powers of singularity γ and β at the point of intersection of the crack and the interface corresponding to a crack terminating at the interface ($a=h_1$, $d<h_2$), and that crossing the interface ($a=h_1$, $d=h_2$, $c>0$), respectively (Figure 1). Unlike the isotropic materials, the characteristic equations (38) and (50) giving γ and β in bonded orthotropic materials are quite complicated. They contain six independent material parameters and hence do not lend themselves to a relatively simple systematic parametric study. However, once the material combination is specified γ and β can be determined quite accurately.

Even though it is very difficult to separate the material parameters which influence most of the values of β and γ , and the stress intensity factors for the imbedded cracks, the calculations show that in this respect perhaps the most important single material parameter is the longitudinal stiffness ratio E_{1yy}/E_{2yy} . In order to assess the effect of the remaining material constants a rather large number of calculations were done by fixing E_{1yy} and E_{2yy} , by systematically varying one at a time the remaining six constants, and by calculating γ , β , and the stress intensity factor $k(a)$, the latter for imbedded cracks in material 1 only. The general trend is as follows: As E_{1xx} , G_{1xy} , and ν_{1xy} (of the medium 1 containing the crack) are increased, γ and $k(a)$ increase, and as E_{2xx} , G_{2xy} , ν_{2xy}

Table 1 Elastic constants of the materials
used in numerical calculations*.

No.	$E_{xx}/$ 10^9N/m^2 (10^6psi)	$E_{yy}/$ 10^9N/m^2 (10^6psi)	$G_{xy}/$ 10^9N/m^2 (10^6psi)	ν_{xy}
1(0)	55.16 (8.0)	170.65 (24.75)	4.83 (0.7)	0.036
2(0)	134.45 (19.5)	31.03 (4.5)	24.13 (3.5)	0.650
3(I)	154.77 (22.447)	155.83 (22.6)	59.68 (8.655)	0.300
4(I)	167.55 (24.3)	170.55 (24.75)	62.40 (9.05)	0.300
5(0)	10.07 (1.46)	31.03 (4.5)	0.833 (0.128)	0.036
6(I)	30.34 (4.4)	31.03 (4.5)	10.83 (1.57)	0.400
7(0)	44.82 (6.5)	155.14 (22.5)	4.83 (0.7)	0.020
8(0)	34.48 (5.0)	6.895 (1.0)	3.45 (0.5)	0.350
9(0)	21.37 (3.1)	66.88 (9.7)	17.93 (2.6)	0.200
10(0)	17.24 (2.5)	17.24 (2.5)	6.895 (1.0)	0.760

(*) The materials are boron-epoxy and graphite-epoxy
with various ply orientations.

Table 2 The power of stress singularity γ for a crack in medium 1 terminating at the interface and β for a crack crossing the interface. The properties of materials used in various combinations are given in Table 1

Comb.	Materials		Power of Sing.		$\frac{E_{1yy}}{E_{2yy}}$	$\frac{G_{1xy}}{G_{2xy}}$
	Med.1	Med.2	γ	β		
I	1	2	0.55048	0	5.50	0.20
II	3	2	0.65699	0.04248	5.02	2.48
III	4	2	0.66549	0.04887	5.50	2.58
IV	4	6	0.68914	0.14547	5.50	5.75
V	4	5	0.80352	0.05354	5.50	70.8
VI	7	8	0.74523	0.05197	22.5	1.40
VII	2	1	0.42258	0	0.182	5.00
VIII	2	3	0.36911	0.04248	0.199	0.403
IX	9	10	0.61554	0.08520	3.88	2.6
X	10	9	0.43410	0.08520	0.268	0.384

ORIGINAL PAGE IS
OF POOR QUALITY

are increased, γ and $k(a)$ decrease. Among these variables the most significant factor influencing γ and $k(a)$ appears to be the ratio of shear moduli G_{1xy}/G_{2xy} . This may partly be observed also from Table 2 and Figure 2. The figure shows the stress intensity factor $k(a)$ for imbedded cracks in material 1 as a function of the width ratio h_2/h_1 for a fixed relative crack length $a/h_1=0.8$ and for material combinations I, III, IV, and V given in Table 2. For these material pairs the stiffness ratio E_{1yy}/E_{2yy} is constant whereas G_{1xy}/G_{2xy} is 0.2, 2.58, 5.75 and 70.8, respectively. It is seen that $k(a)$ is consistently higher in material pairs having the greater G_{1xy}/G_{2xy} ratio. Figure 2 also shows that for $h_2 \rightarrow 0$, as expected, in all material combinations $k(a)$ approaches the periodic collinear crack solution in an infinite plane which is the same for all homogeneous orthotropic as well as isotropic materials.

A close examination of the results giving β , γ , and $k(a)$ indicates that generally one could accomplish a certain relaxation in the stress singularity at the point of intersection of a crack and an interface in composites by introducing orthotropic materials. This may be seen, for example, by comparing the β values for various material combinations given in Table 2. In fact for certain orthotropic material combinations it is even possible to have $\beta=0$, i.e., no singularity, whereas in isotropic materials β is always positive, i.e., the stress state is always singular. The value of β has, of course, an important bearing on the initiation of a possible delamination fracture from the stress-free boundaries in bonded materials. Even though the result regarding the possibility of $\beta=0$ may appear to be somewhat paradoxical, considering the fact that in two isotropic wedges forming a half plane β is dependent on the wedge angles as well as the material constants and may be zero for certain ranges of wedge angles, it should not be completely unexpected. The possibility of reduction or complete elimination of singularity power β by varying the

secondary material constants seems to introduce an added flexibility in designing against the edge delamination in bonded materials.

In solving the integral equations it is assumed that the composite medium is under a state of generalized plane stress and is subjected to external loads away from and perpendicular to the cracks. Thus the crack surface tractions in the perturbation problem considered in this paper are constant and are at the following ratio:

$$\frac{p_1(x)}{p_2(x)} = \frac{-p_1}{-p_2} = \frac{E_{1yy}}{E_{2yy}} . \quad (65)$$

The stress intensity factors obtained for the imbedded cracks located in the first or second set of strips are given in Figures 3-7. Comparison of the results given in Figures 3 and 4 shows that for the same longitudinal stiffness ratio E_{1yy}/E_{2yy} and the same material 2, $k(a)$ calculated for an isotropic medium 1 is consistently greater than that calculated for an orthotropic material 1. This means that by introducing material orthotropy it is possible to obtain certain relaxation in the stress intensity factor. However, as seen from Figure 2, due to the effect of the secondary material parameters the opposite is also possible. In Figure 2 note that the combination IV refers to an isotropic-isotropic material pair - whereas III and V are isotropic-orthotropic pairs giving stress intensity factors which are respectively lower and higher than that of IV. Corresponding results for the stress intensity factor $k(b)$ for cracks imbedded in the second medium are given in Figures 6 and 7. Materials in Figures 5 and 7 are of the type II and those in Figures 2, 3, 4 and 6 are of type I. It should be observed that as the thickness of the uncracked strips go to zero, the stress intensity factor in the cracked strips approach that of the periodic crack problem in the infinite homogeneous (isotropic or orthotropic) medium.

Figure 8 shows a sample result for a composite medium in which both sets of strips contain cracks. Additional results for two as well as one set of cracks may be found in [14] and [15].

The stress intensity factors for the case of a broken laminate (i.e., for $a=h_1$ and $c=d$, or $a=0$ and $d=h_2$, $c=0$) are given in Figures 9-12. Figures 9 and 10 show the results for material combinations I and II where all materials are of type I and Figures 11 and 12 give an example for the material combination IX where both materials are of type II. The figures show that in all cases as the width of the uncracked strip (i.e., the net ligament between the cracks) goes to zero, as expected, the stress intensity factors become unbounded. In these problems the stress intensity factor is defined by (42) and is calculated from (43).

The results for a crack crossing the interface are given in Figures 13-19. In these problems the stress intensity factor at the crack tip $k(c)=k_b$ is defined by and calculated from (29b). For those material combinations in which $\beta>0$ the stress intensity factors at the point of intersection of the crack and the interface k_{xx} and k_{xy} are defined by (61) and are calculated from (62). For the material combinations II, IX and I used in these examples, Table 2 shows that power of stress singularity γ for a crack in material 1 touching the interface is greater than $1/2$. Therefore, as the crack length $2a$ approaches $2h_1$ or as $c \rightarrow h_2$, the stress intensity factor k_b at the crack tip calculated on the basis of $1/2$ power becomes unbounded. Also, as the length of the net ligament $2c$ goes to zero k_b again becomes unbounded. These features of the solution may be observed from Figures 13, 16, and 19 giving the crack tip stress intensity factor as a function c/h_2 . Figures 13 and 16 show k_b for material combinations II and IX in which $\beta>0$. Figure 19 gives an example for the case in which $\beta=0$. It may be noted that qualitatively the results for the two cases are quite similar.

The stress intensity factors k_{xx} and k_{xy} for material combinations II and IX are given in Figures 14, 15, 17, and 18. Note that in the limiting case of $c=h_2$, that is for the case of the crack touching the interface, the power of the stress singularity at the interface would be γ which is always greater than β . Therefore, as expected and as seen from the figures, for $c \rightarrow h_2$ the stress intensity factors calculated on the basis of singularity power β become unbounded. In these problems for the type of loading under consideration the normal component k_{xx} of the stress intensity factor seems to be negative. Since there is no crack surface interference, physically this means that normal stress along the interface near the crack surface is compressive, there is no inconsistency, and the singularity should be interpreted in the same way as in punch problems.

REFERENCES

1. F. Erdogan, "Fracture problems in composite materials," J. Engng. Fracture Mechanics, Vol. 4, pp. 811-840 (1972).
2. F. Erdogan, "Fracture of nonhomogeneous solids," The Mechanics of Fracture, AMD Vol. 19, pp. 155-170, ASME, New York (1976).
3. D. D. Ang and M. L. Williams, "Combined stresses in an orthotropic plate having a finite crack," J. Applied Mech., Vol. 28, Trans. ASME, pp. 372-378 (1961).
4. G. N. Savin, Stress Concentration Around Holes, Pergamon Press, New York (1961).
5. G. C. Sih, P. C. Paris, and G. R. Irwin, "On cracks in rectilinearly anisotropic bodies," Int. J. Fracture Mechanics, Vol. 1, pp. 189-203 (1965).
6. S. Krenk, "Stress distribution in an infinite anisotropic plate with collinear cracks," Int. J. Solids and Structures, Vol. 11, pp. 449-460 (1975).
7. D. L. Clements, "A crack between dissimilar anisotropic media," Int. J. Engng. Sci., Vol. 9, pp. 257-265 (1971).

8. F. Delale and F. Erdogan, "The problem of internal and edge cracks in an orthotropic strip," J. Appl. Mech., Vol. 44, Trans. ASME, pp. 237-242 (1977).
9. K. Arin, "A note on the fracture of laminated composites," Letters in Applied and Engineering Sciences, Vol. 3, pp. 81-85 (1975).
10. F. Erdogan and M. Bakioglu, "Fracture of plates which consist of periodic dissimilar strips," Int. J. of Fracture, Vol. 12, pp. 71-84 (1976).
11. F. Erdogan and M. Bakioglu, "Stress-free end problem in layered materials," Int. J. of Fracture, Vol. 13, pp. 739-749 (1977).
12. M. R. Gecit and F. Erdogan, "The effect of adhesive layers on the fracture of laminated structures," J. of Engineering Materials and Technology, Trans. ASME, Vol. 100, pp. 2-9 (1978).
13. S. G. Lekhnitskii, Anisotropic Plates, Gordon & Breach, New York (1968).
14. F. Delale, "Fracture of Composite Orthotropic Plates Containing Periodic Buffer Strips," Ph.D. Dissertation, Lehigh University (1976).
15. F. Delale, "Fracture of composite orthotropic plates for materials type II," Technical Report NASA Grant NGR 39-007-011 (1976).
16. F. Erdogan, "Mixed boundary value problems in mechanics," Mechanics Today, S. Nemat-Nasser, Ed., Vol. 4, pp. 1-86 (1978).
17. F. Erdogan and V. Biricikoglu, "Two bonded half planes with a crack going through the interface," Int. J. Engng. Sci., Vol. 11, pp. 745-766 (1973).
18. T. S. Cook and F. Erdogan, "Stresses in bonded materials with a crack perpendicular to the interface," Int. J. Engng. Sci., Vol. 10, pp. 667-697 (1972).

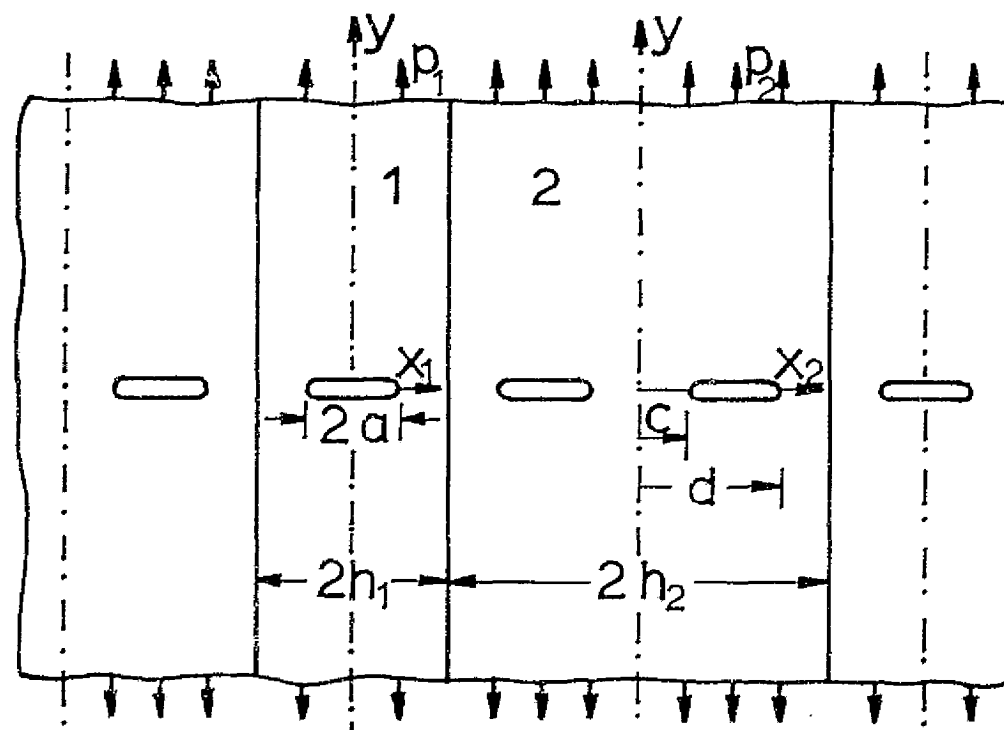


Figure 1 Crack geometry for periodically arranged bonded orthotropic strips

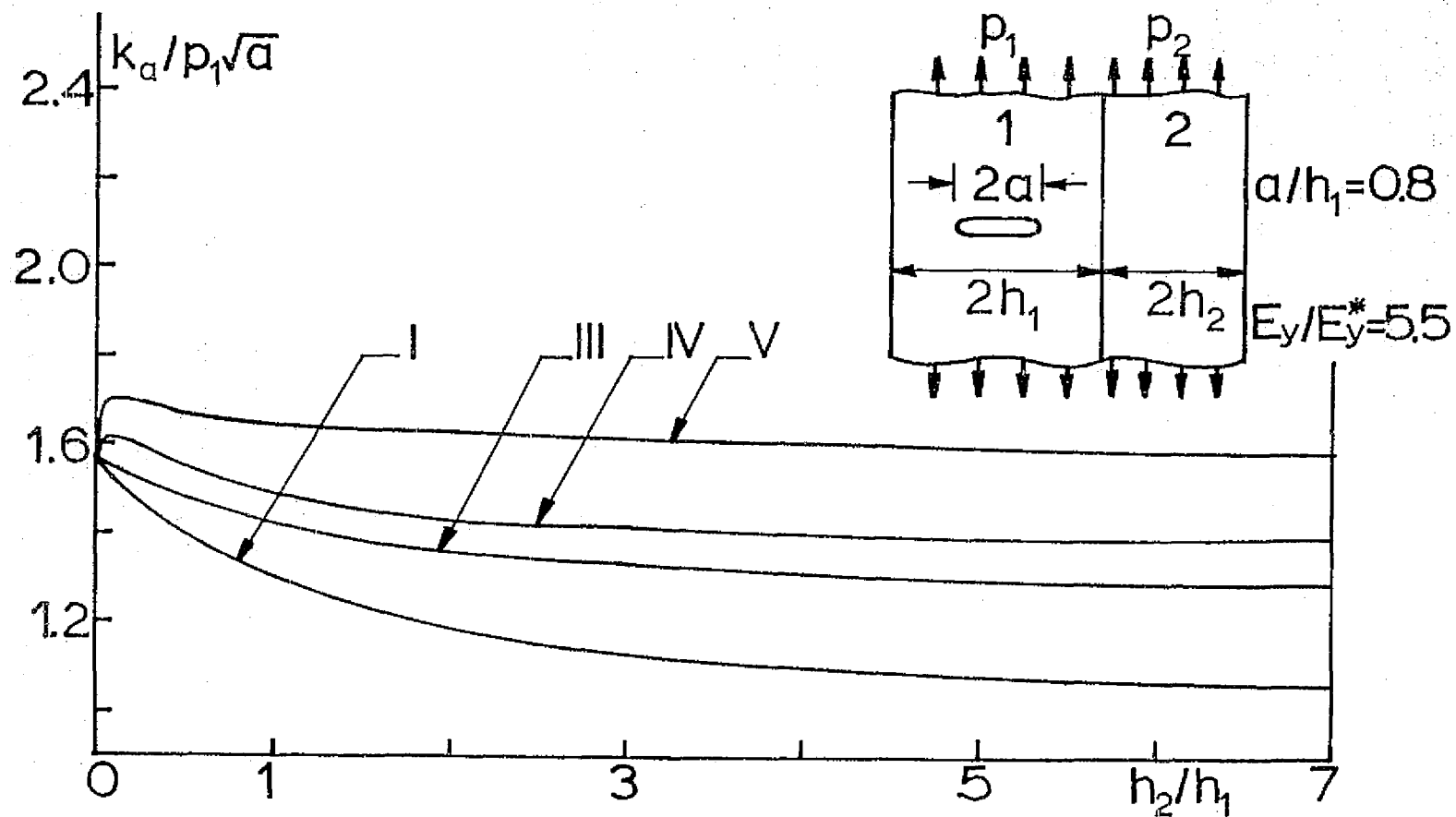


Figure 2 Stress intensity factor $k(a)=k_a$ for cracks imbedded in strip I ($0 < a < h_1$, $b=d=c$) for material combinations I, III, IV and V. $E_y=E_{1yy}$, $E_y^*=E_{2yy}$, $a/h_1=0.8$ =constant

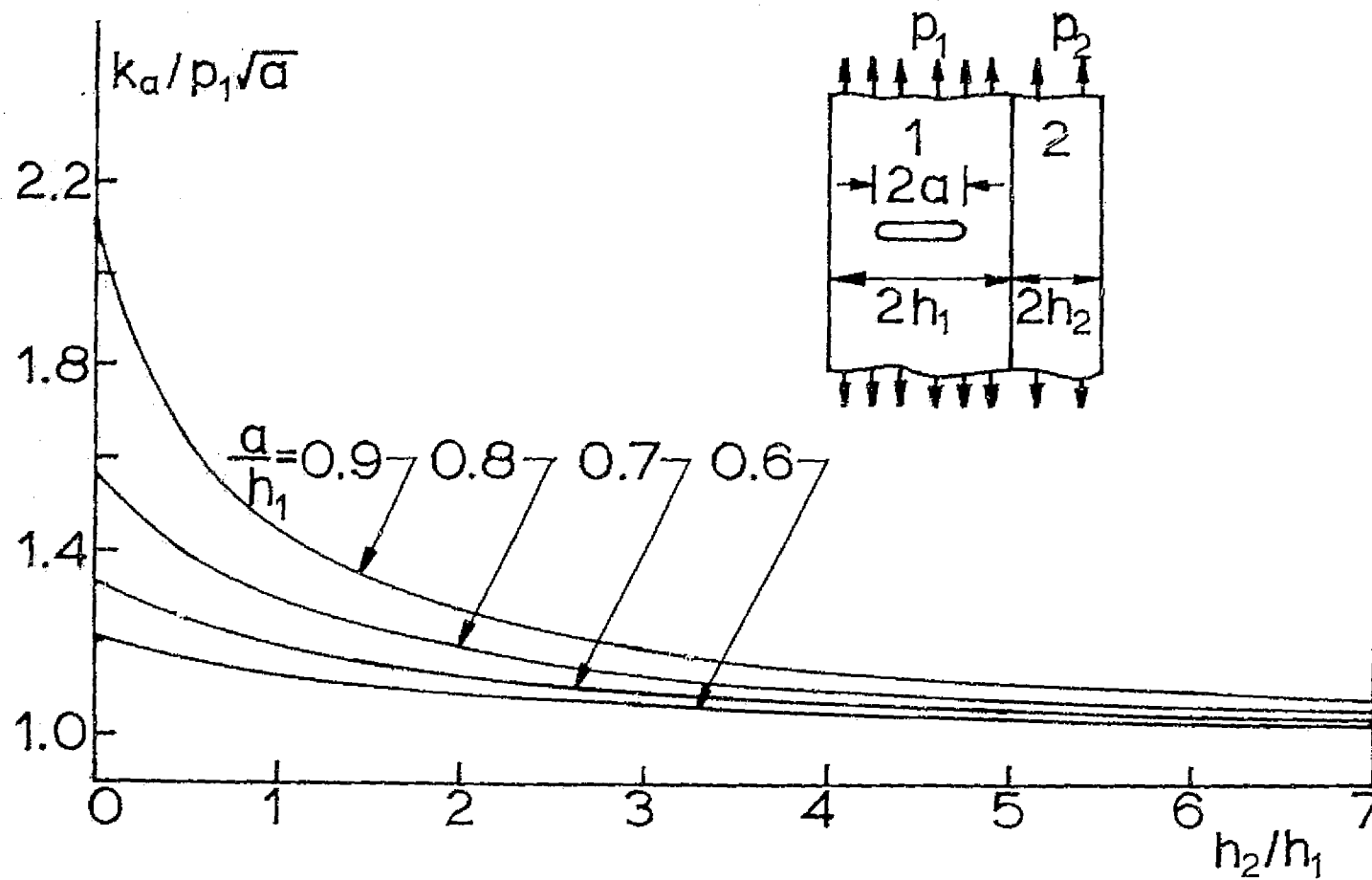


Figure 3 Stress intensity factor $k(a)=k_a$ for cracks imbedded in strip 1 for material combination I

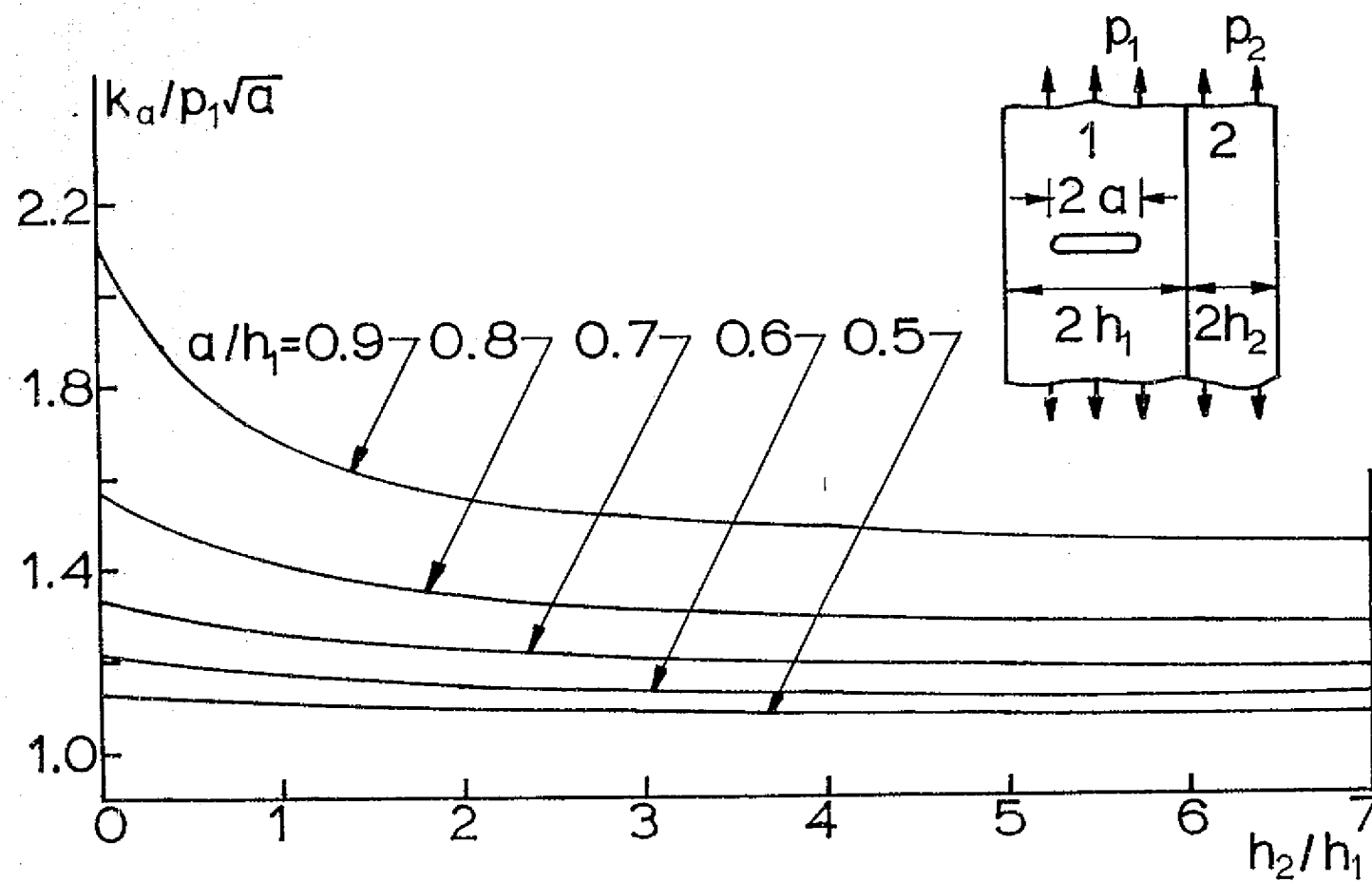


Figure 4 Same as Figure 3 for material combination II

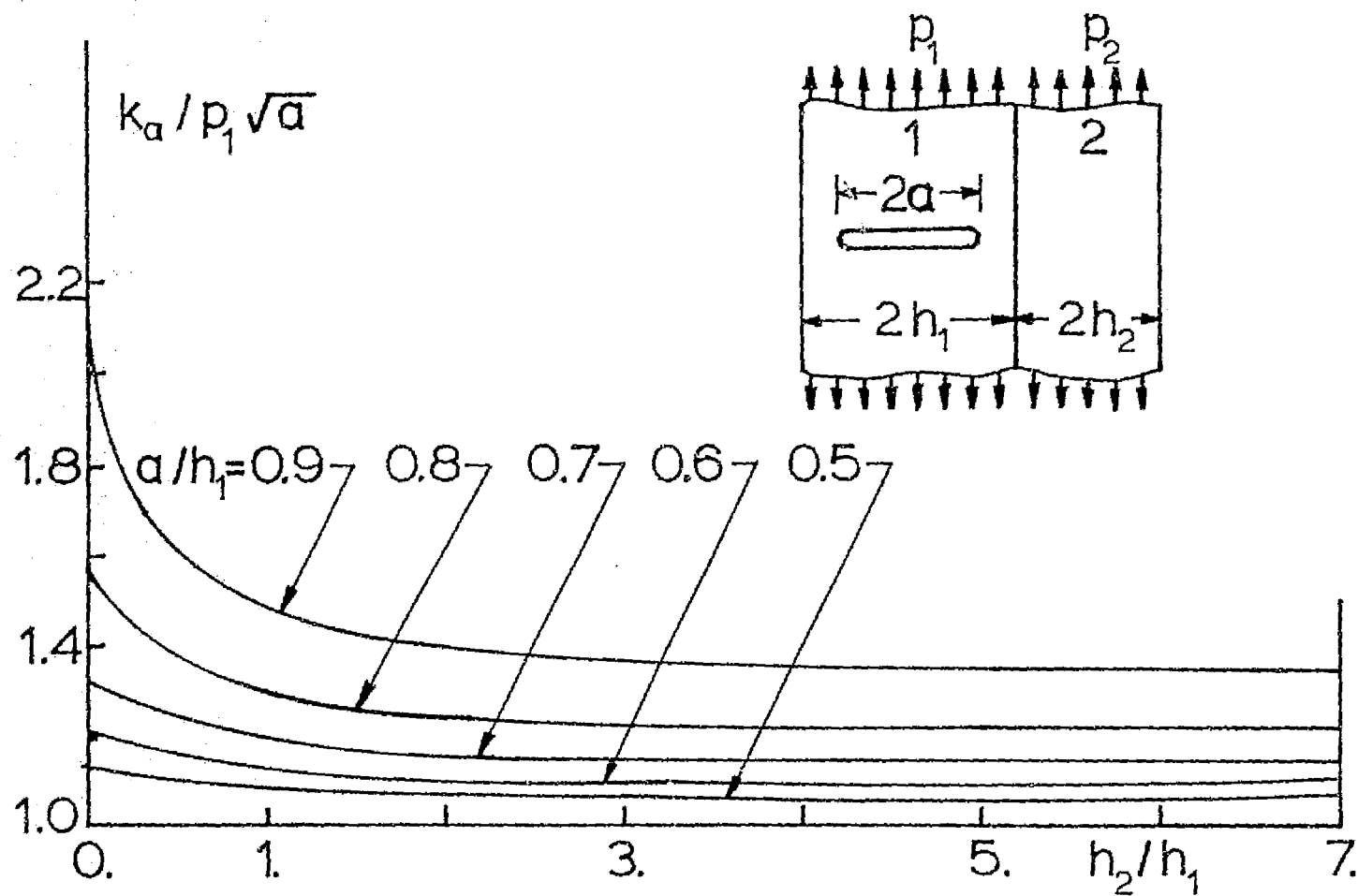


Figure 5 Same as Figure 3 for material combination IX

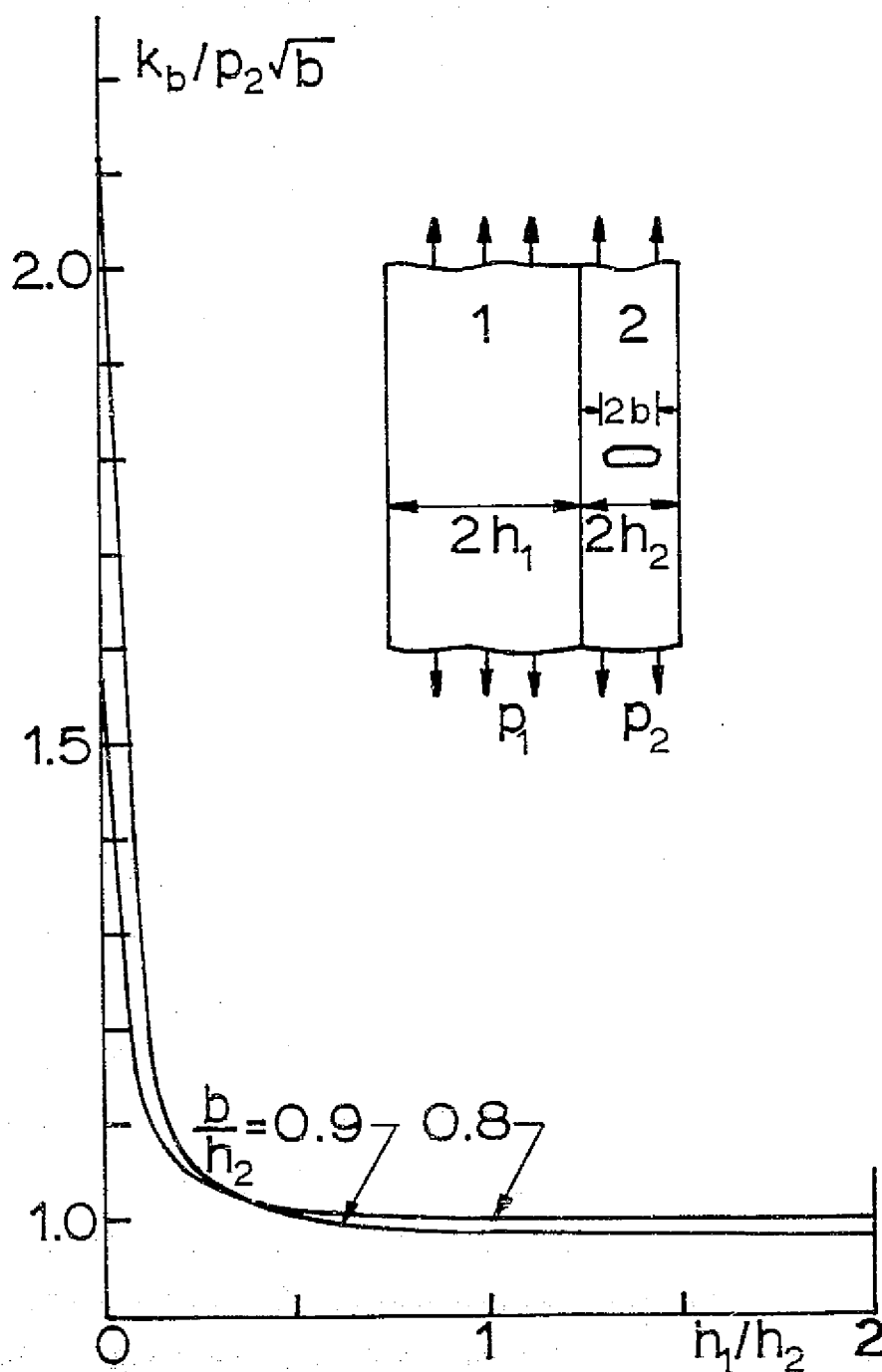


Figure 6 Stress intensity factor $k_b=k(b)$ for cracks imbedded in strip 2 ($a=0$, $c=0$, $d=b<h_2$) for material combination I

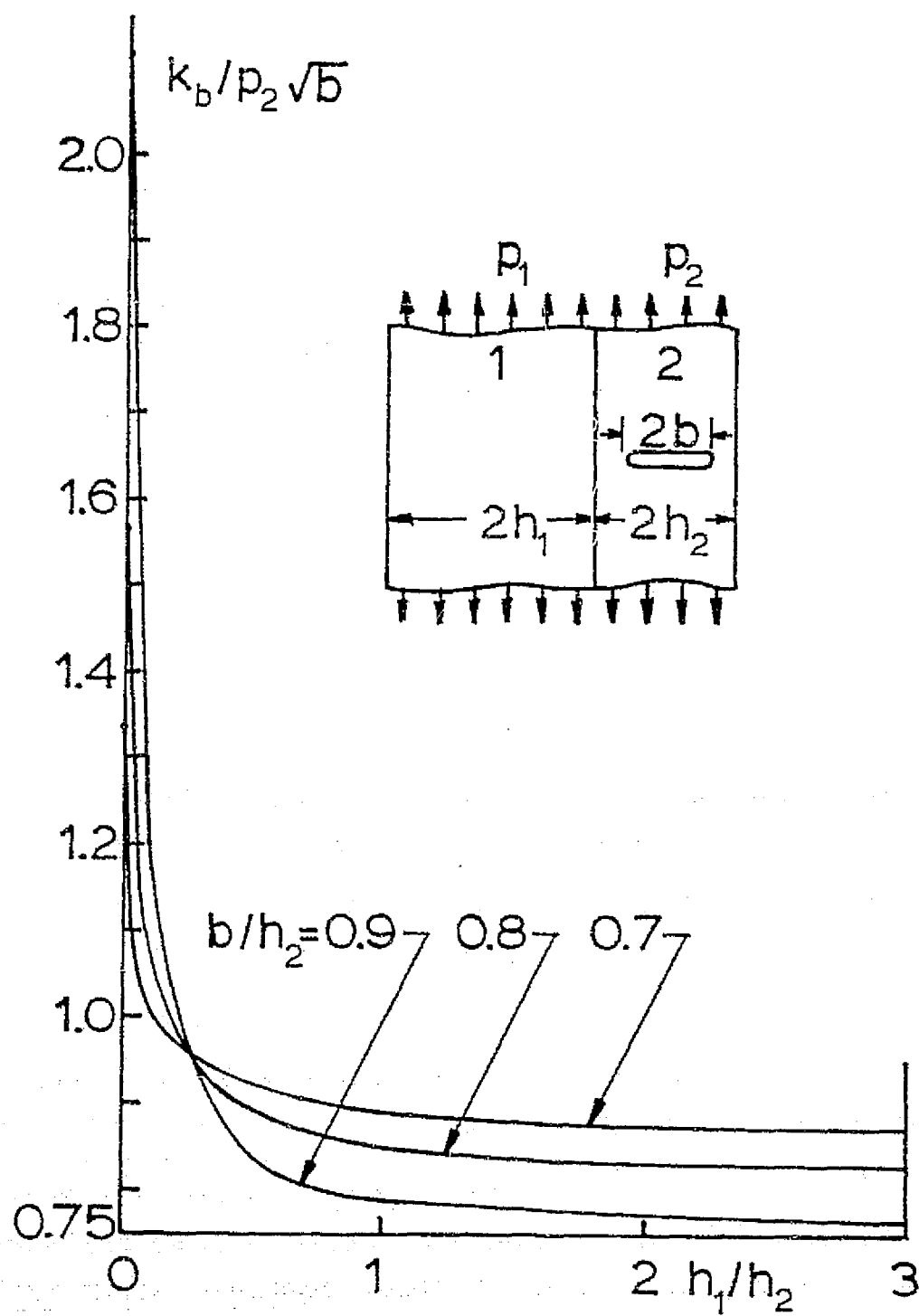


Figure 7 Same as Figure 6 for material combination IX

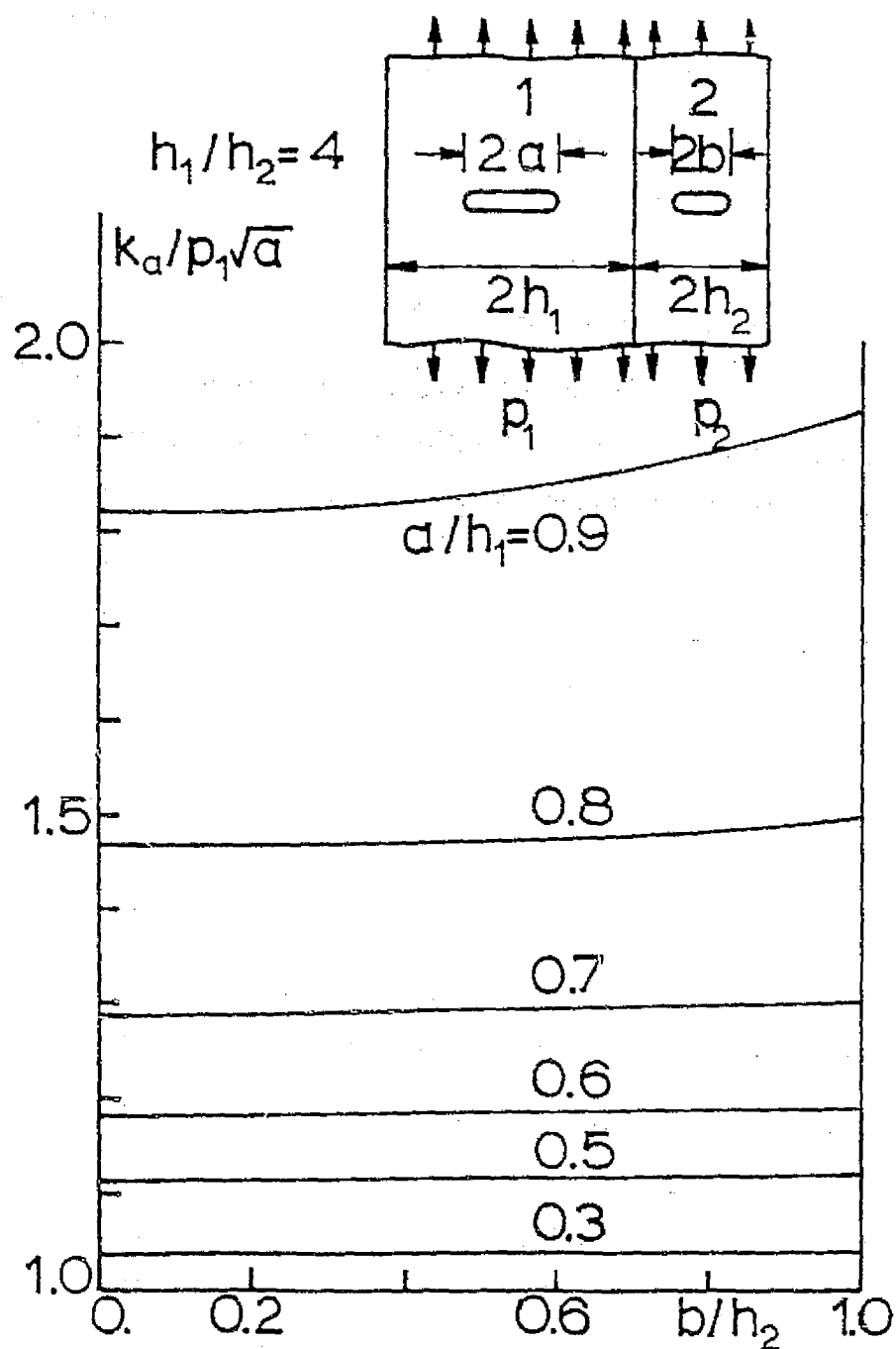


Figure 8 Stress intensity factor $k(a)=k_a$ for the crack in material 1 in a composite medium where both sets of strips contain cracks. Material combination I, width ratio $h_1/h_2=4$

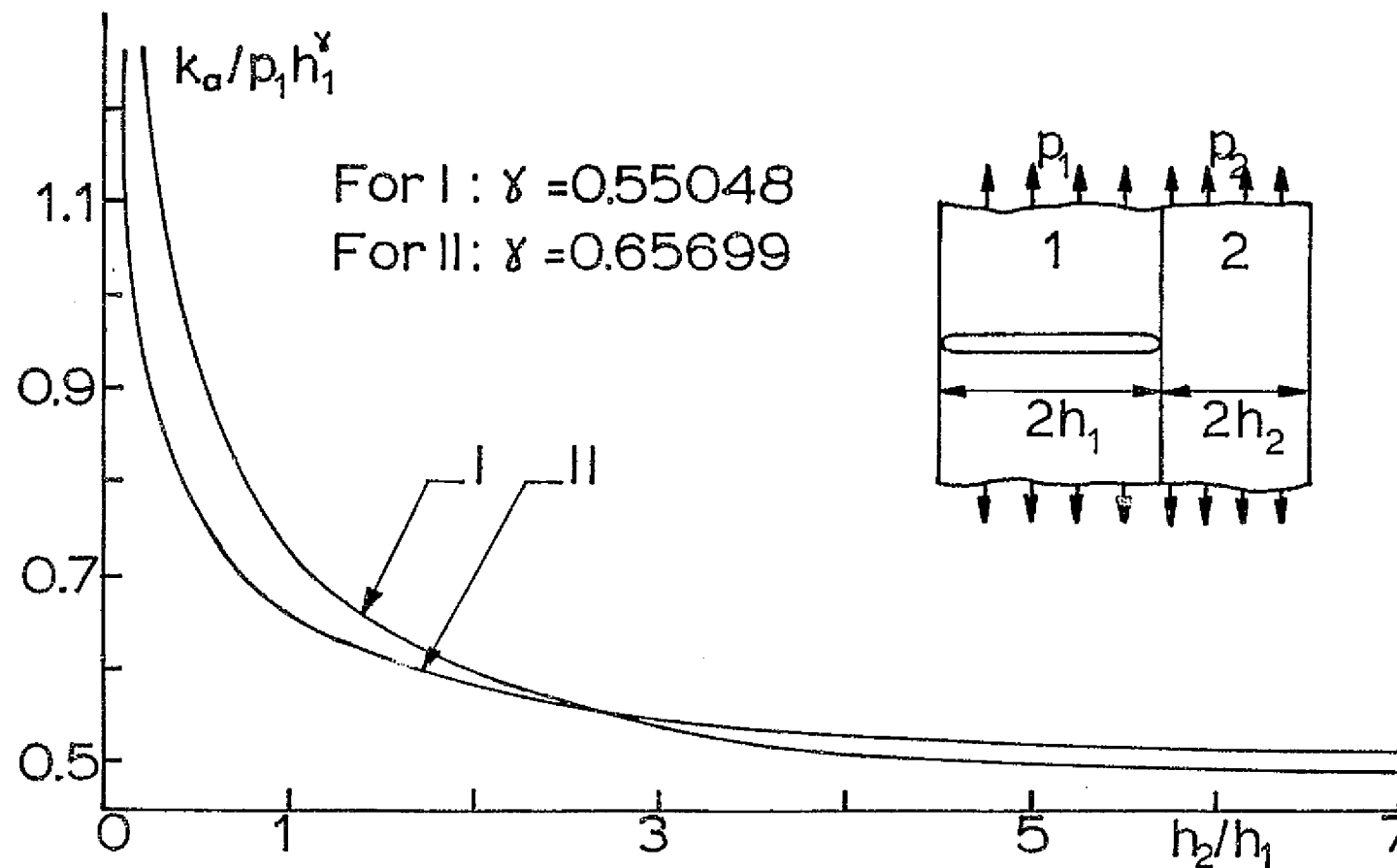


Figure 9 The stress intensity factor $k(h_1) = k_a$ for broken laminates 1 in material combinations I and II

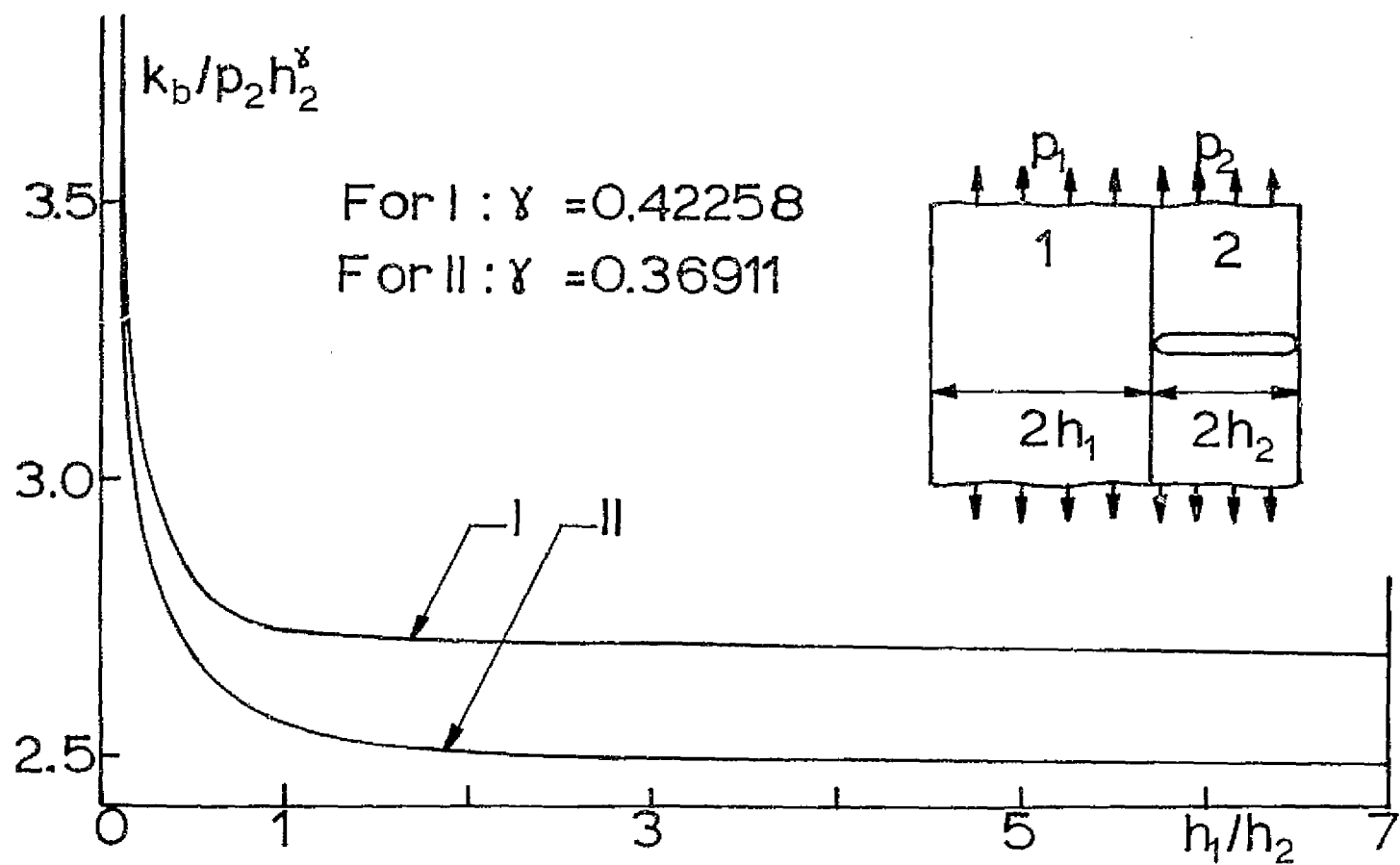


Figure 10 The stress intensity factor $k(h_2)=k_b$ for broken laminates 2 in material combinations I and II

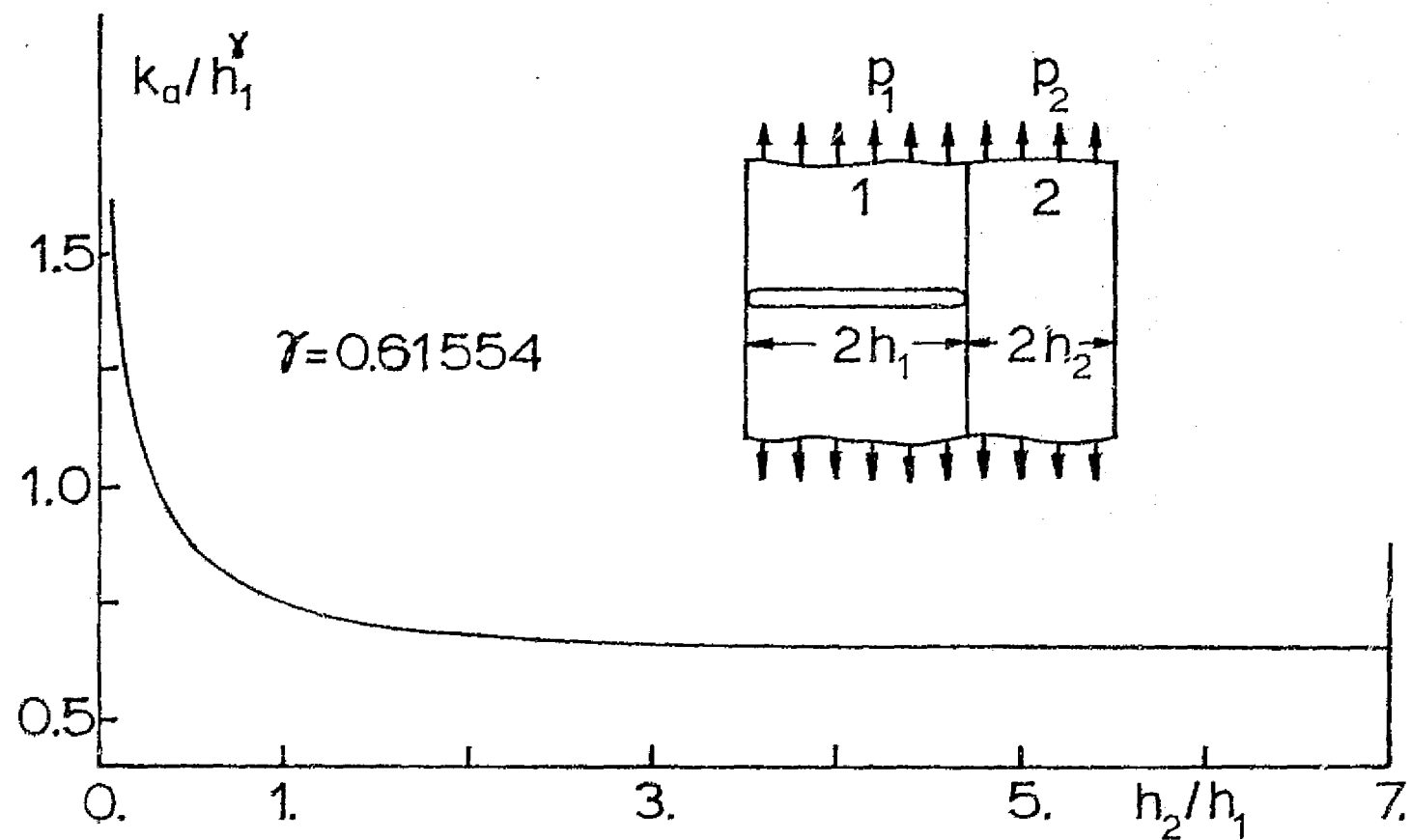


Figure 11 Same as Figure 9, material combination IX

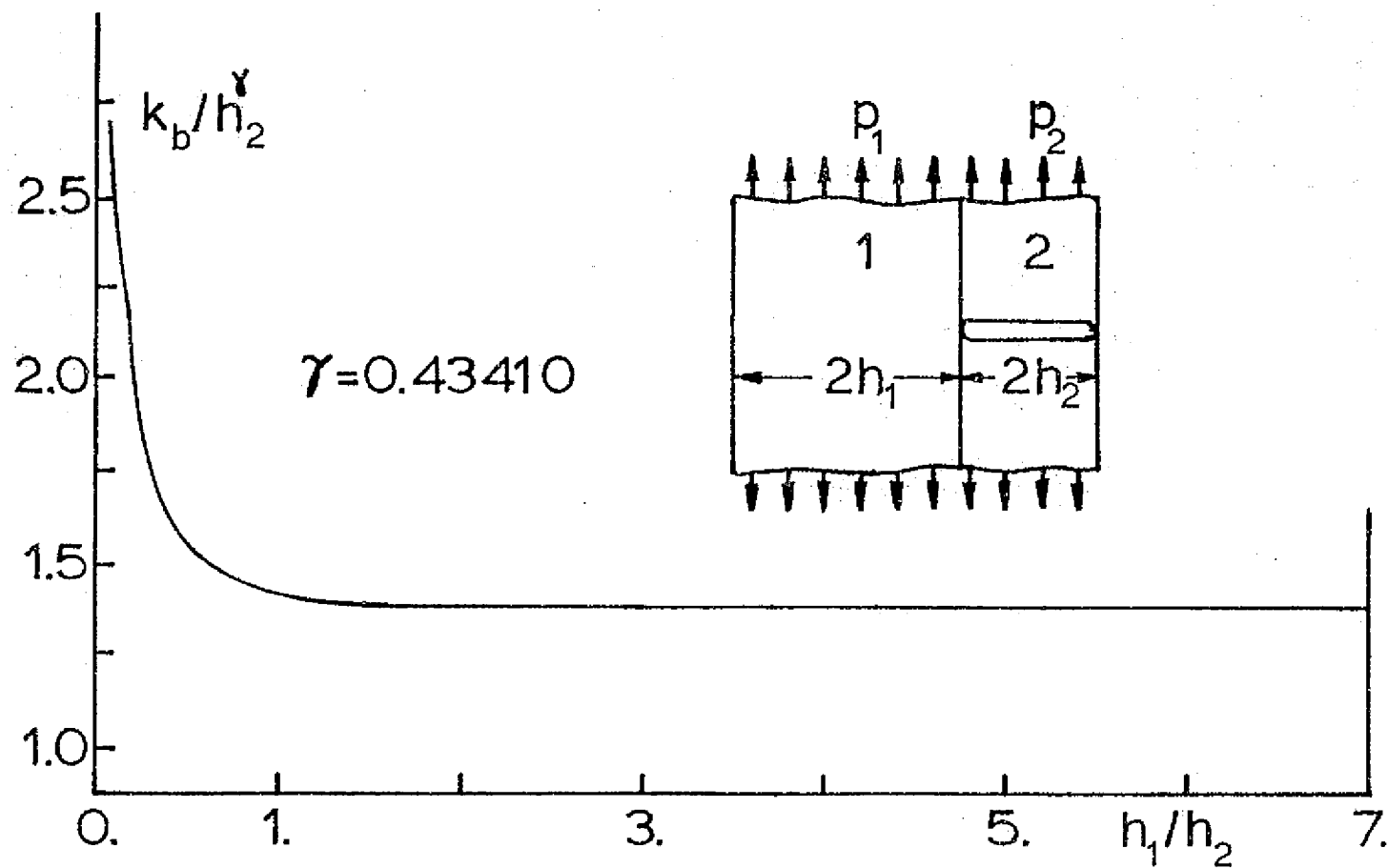


Figure 12 Same as Figure 10, material combination IX.

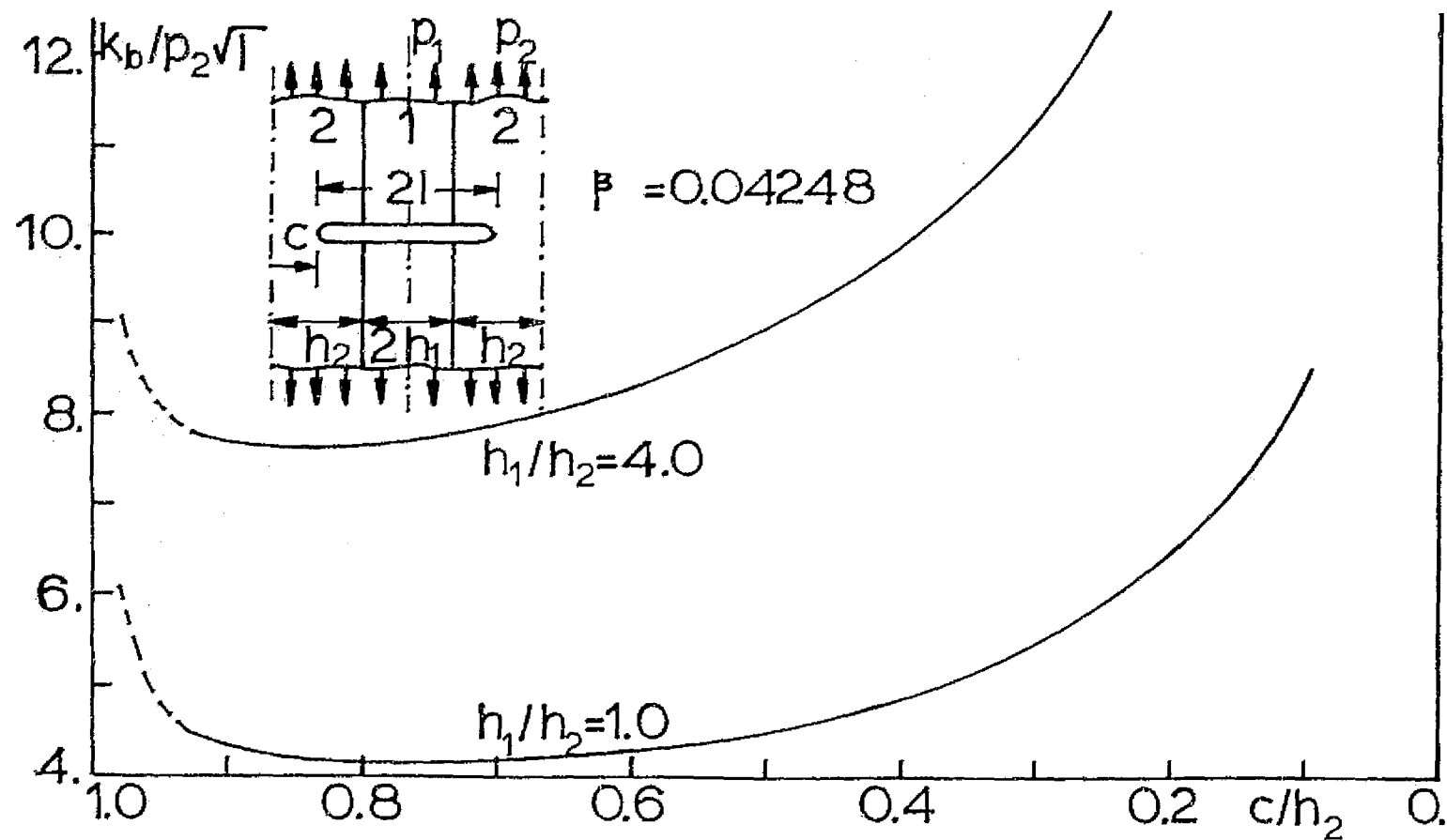


Figure 13 The stress intensity factor at the crack tip $k(c)=k_b$ for cracks crossing the interface in material combination II

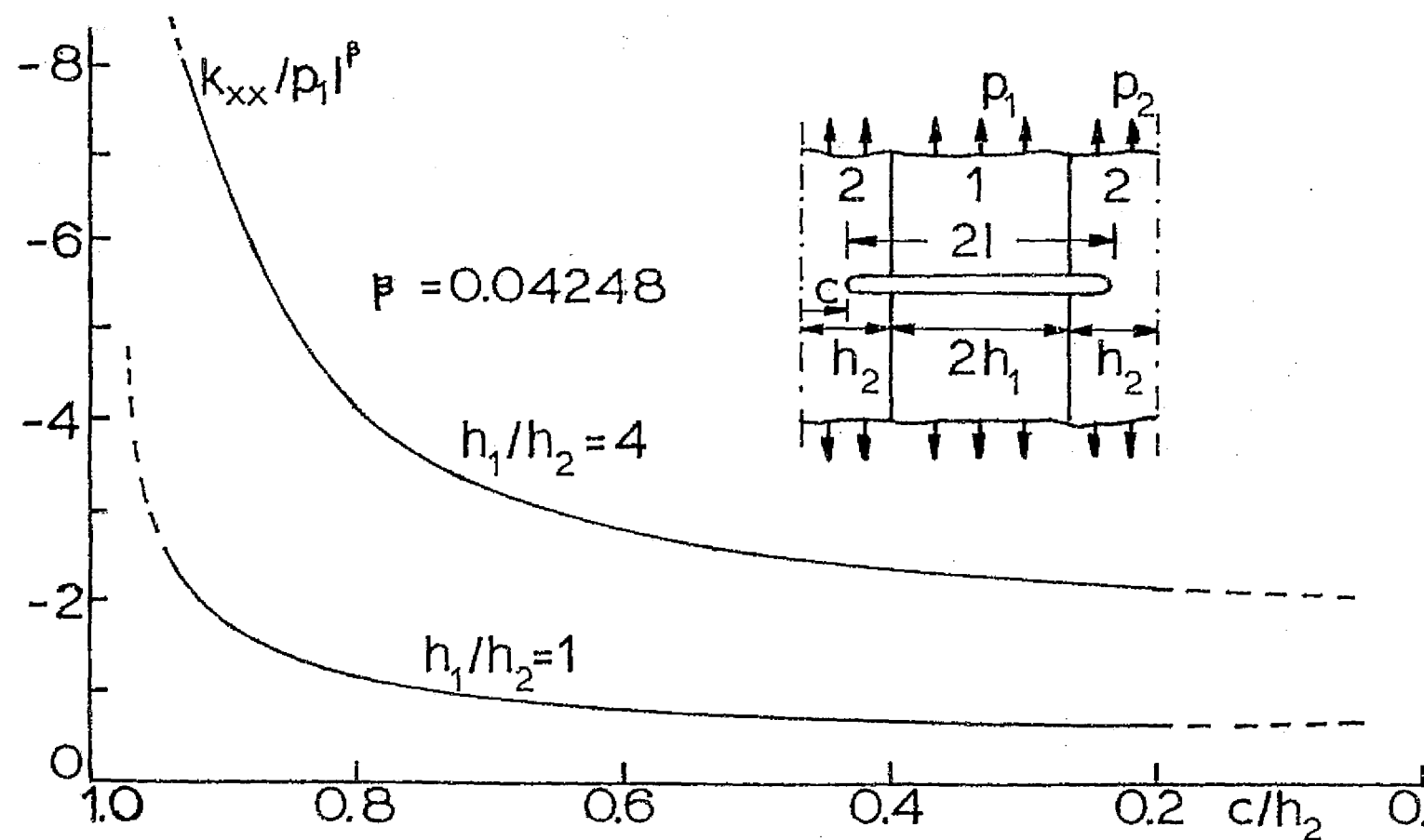


Figure 14 Normal component k_{xx} of the stress intensity factor at the intersection of the cracks and the interfaces in material combination II

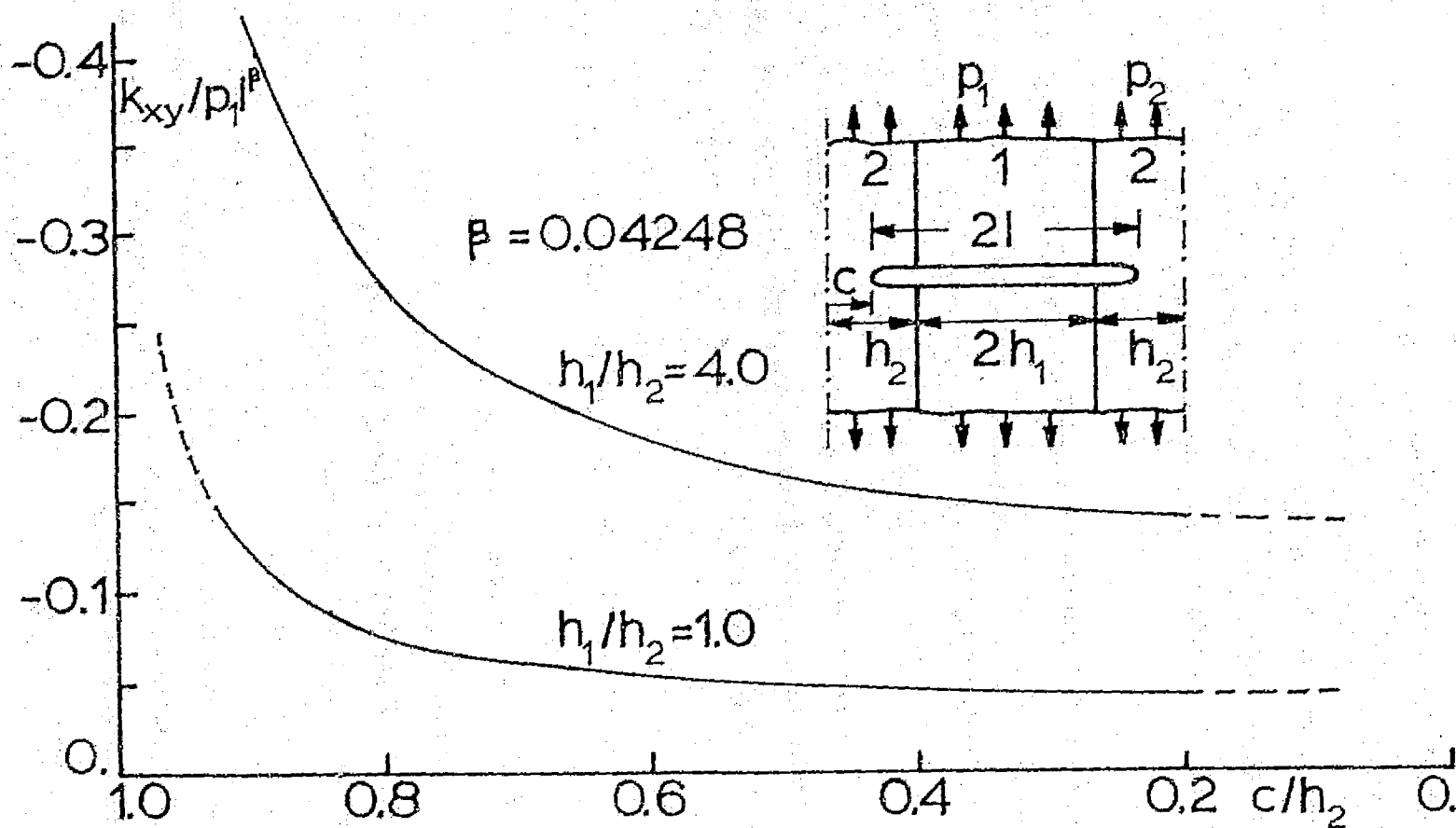


Figure 15 Shear component k_{xy} of the stress intensity factor at the intersection of the cracks and the interfaces in material combination II

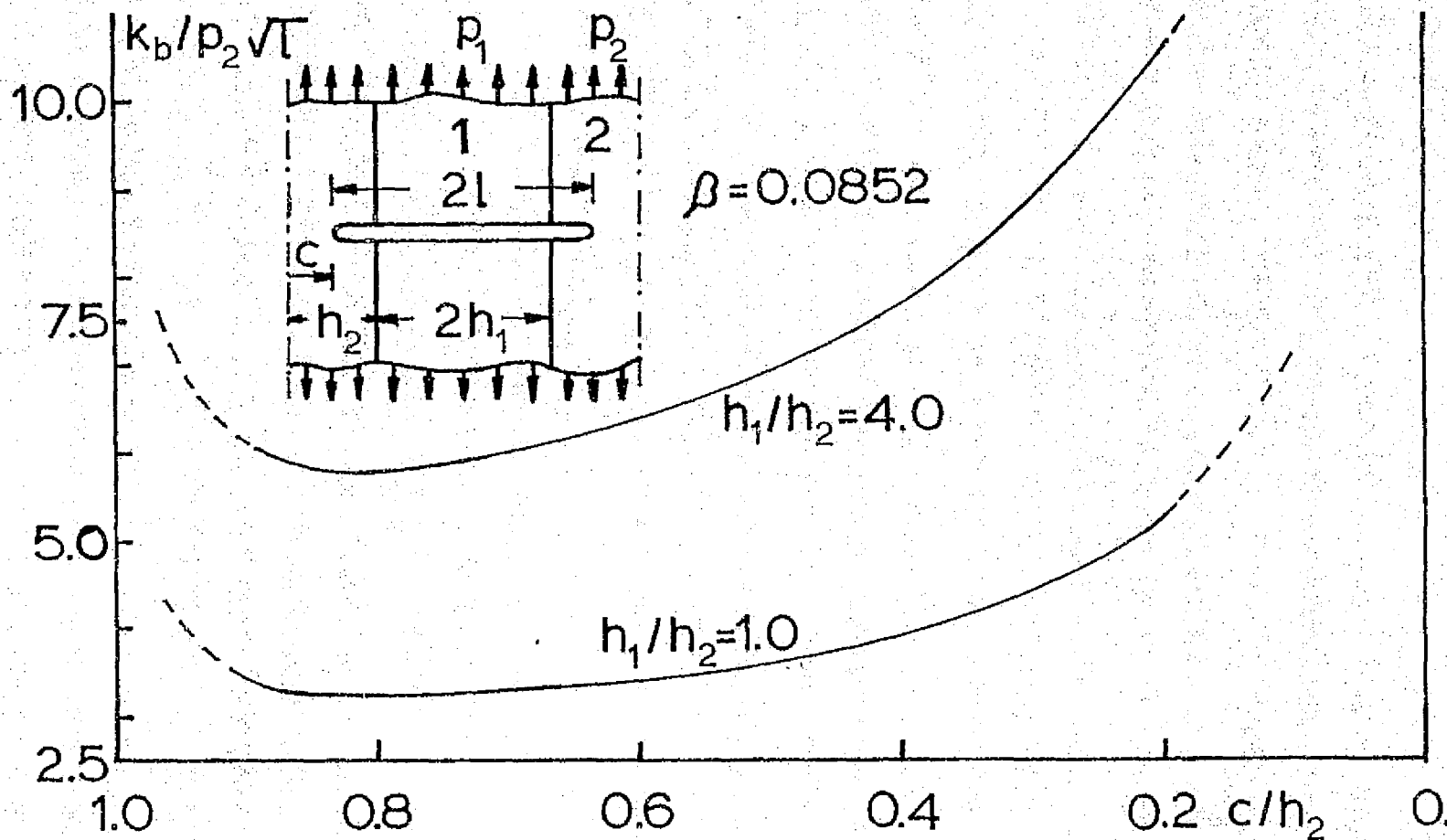


Figure 16 Same as Figure 13 in material combination IX

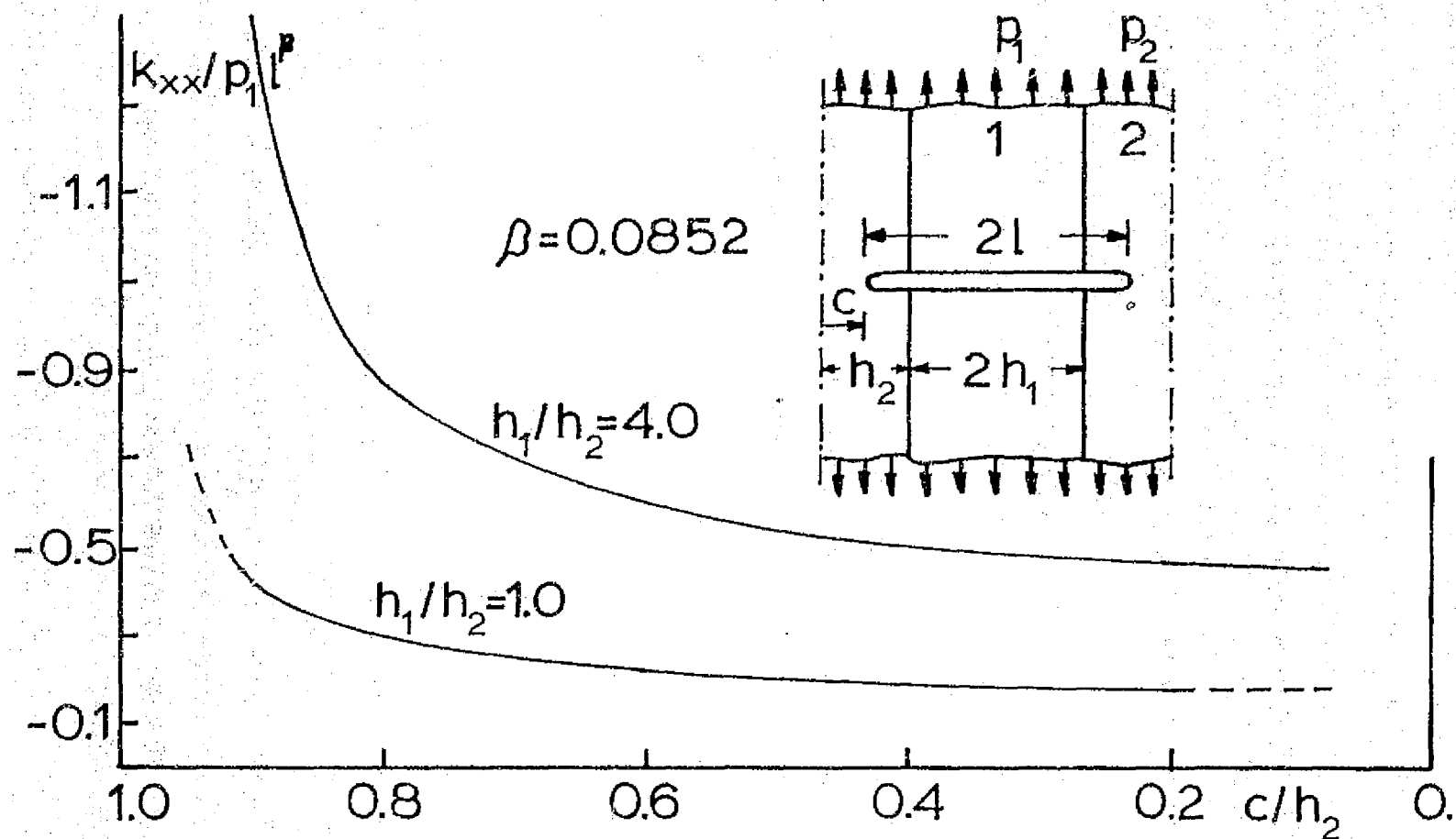


Figure 17 Same as Figure 14 in material combination IX

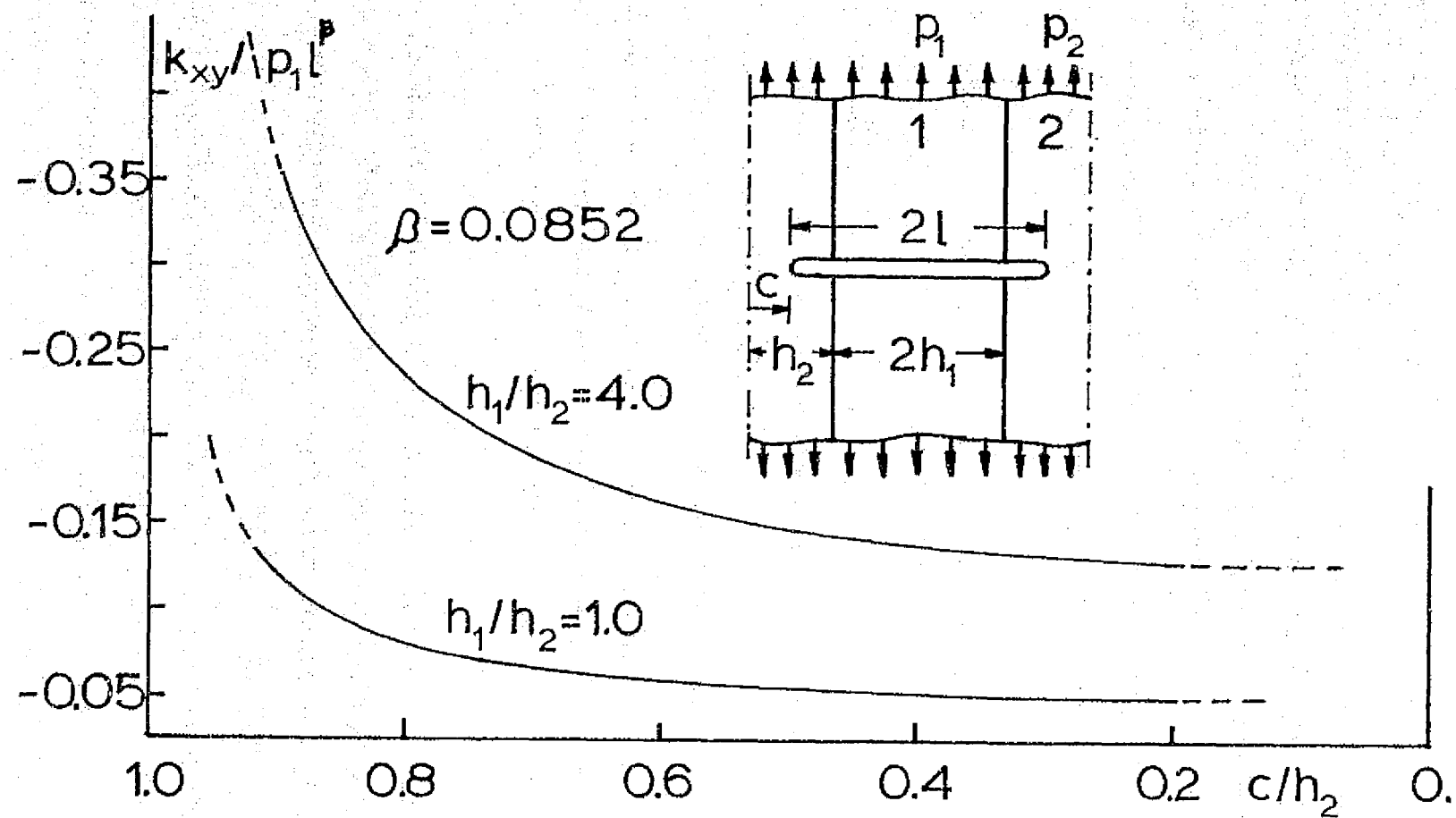


Figure 18 Same as Figure 15 in material combination IX

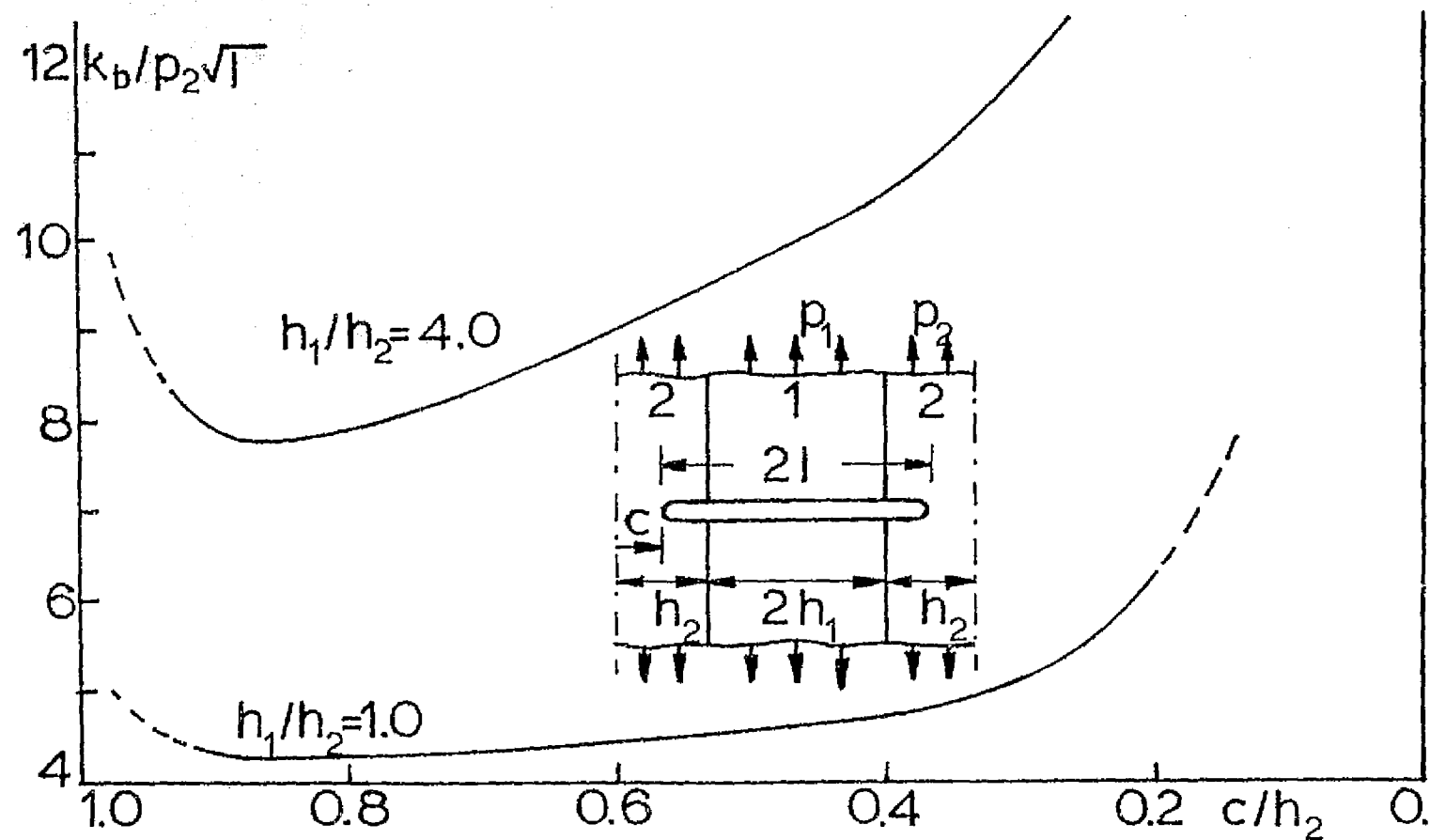


Figure 19 Same as Figure 13 in material combination I where $\beta=0$